



### **Science Arts & Métiers (SAM)**

is an open access repository that collects the work of Arts et Métiers Institute of Technology researchers and makes it freely available over the web where possible.

This is an author-deposited version published in: <https://sam.ensam.eu>  
Handle ID: <http://hdl.handle.net/10985/8952>

#### **To cite this version :**

Mélodie MONTEIL, Cyril TOUZÉ, Olivier THOMAS, Simon BENACCHIO - Nonlinear forced vibrations of thin structures with tuned eigenfrequencies: the cases of 1:2:4 and 1:2:2 internal resonances - Nonlinear Dynamics - Vol. 75, n°1-2, p.175-200 - 2014

Any correspondence concerning this service should be sent to the repository

Administrator : [scienceouverte@ensam.eu](mailto:scienceouverte@ensam.eu)



---

# Nonlinear forced vibrations of thin structures with tuned eigenfrequencies: the cases of 1:2:4 and 1:2:2 internal resonances

Mélie Monteil · Cyril Touzé · Olivier Thomas ·  
Simon Benacchio

**Abstract** This paper is devoted to the analysis of nonlinear forced vibrations of two particular three degrees-of-freedom (dofs) systems exhibiting second-order internal resonances resulting from a harmonic tuning of their natural frequencies.

The first model considers three modes with eigenfrequencies  $\omega_1$ ,  $\omega_2$ , and  $\omega_3$  such that  $\omega_3 \simeq 2\omega_2 \simeq 4\omega_1$ ,

thus displaying a 1:2:4 internal resonance. The second system exhibits a 1:2:2 internal resonance, so that the frequency relationship reads  $\omega_3 \simeq \omega_2 \simeq 2\omega_1$ . Multiple scales method is used to solve analytically the forced oscillations for the two models excited on each degree of freedom at primary resonance. A thorough analytical study is proposed, with a particular emphasis on the stability of the solutions. Parametric investigations allow to get a complete picture of the dynamics of the two systems. Results are systematically compared to the classical 1:2 resonance, in order to understand how the presence of a third oscillator modifies the nonlinear dynamics and favors the presence of unstable periodic orbits.

**Keywords** Internal resonance · Nonlinear oscillations · Multiple scales

---

M. Monteil · C. Touzé (✉)  
Unité de Mécanique (UME), ENSTA-ParisTech,  
828 Boulevard des Maréchaux, 91762 Palaiseau Cedex,  
France  
e-mail: [cyril.touze@ensta-paristech.fr](mailto:cyril.touze@ensta-paristech.fr)

M. Monteil  
e-mail: [melodie.monteil@ensta-paristech.fr](mailto:melodie.monteil@ensta-paristech.fr)

M. Monteil  
Institut Jean Le Rond d'Alembert, UPMC-Paris VI/CNRS,  
4 place Jussieu, 75252 Paris Cedex 05, France

O. Thomas  
Structural Mechanics and Coupled Systems Laboratory,  
Conservatoire National des Arts et Métiers (CNAM),  
2 rue Conté, 75003 Paris, France  
e-mail: [olivier.thomas@ensam.eu](mailto:olivier.thomas@ensam.eu)

O. Thomas  
Laboratoire des Sciences de l'Information et des Systèmes  
UMR 7296, Arts et Métiers ParisTech, 8 Boulevard  
Louis XIV, 59000 Lille, France

S. Benacchio  
IRCAM, CNRS UMR 9912, UPMC, 1 Place Igor  
Stravinsky, 75004 Paris, France  
e-mail: [benacchio@ircam.fr](mailto:benacchio@ircam.fr)

## 1 Introduction

Nonlinear resonances in the field of nonlinear vibrations have been recognized since a long time as a major effect that complexifies the nonlinear dynamics by creating strong energy exchange between modes (see, e.g., [23, 24] and references therein). In turn, these strong couplings increase the number of excited modes in a given dynamical response, and thus make the appearance of complex solutions more probable, including quasiperiodicity and chaos, following for instance the Ruelle–Takens scenario [30]. Today, these

general ideas still find applications in the comprehension of the transition scenario to turbulence in vibrating plates [36], as well as in the description of wave turbulence regime, dominated by N-waves nonlinear interactions [26].

For moderately nonlinear vibrations, internal resonances occur for structures displaying a simple (commensurable) relationship between its eigenfrequencies, in the line of the normal form theory [13, 23, 29, 38]. A particular case is the now well-documented 1:2 resonance relationship, where two eigenfrequencies ( $\omega_1, \omega_2$ ) are such that  $\omega_2 \simeq 2\omega_1$ . This second-order internal resonance involves quadratic nonlinearity, and is now classical, since the first report of its effect on the response of a ship system by Froude [10, 22]. References [11, 21, 23, 24, 35] provide a complete picture of analytical solutions and experimental observations. Note that we use here the terminology “1:2” resonance to name that case whereas it is often denoted 2:1 resonance in other studies. Complications to the classical 1:2 case have already been considered as it appears in many physical systems such as strings, cables, plates, and shells. Lee and Perkins [16] reported a study on a 1:2:2 resonance occurring in suspended cables between in-plane and out-of-plane modes, and denoted that resonance as a 2:1:1 case. In their study, only one of the two high-frequency modes was excited, and the coupling with the two other modes was studied. In the field of nonlinear vibrations of shells, multiple cases involving different combinations of 1:1 and 1:2 resonances have been found to occur frequently. Chin and Nayfeh studied the case of a 1:1:2 resonance in a circular cylindrical shell, where only one of the two low-frequency modes were excited [8]. Thomas et al. studied theoretically and experimentally the 1:1:2 resonance occurring in shallow spherical shells, where the driven mode is the high-frequency one [33, 34]. The case of a 1:1:1:2 internal resonance occurring in closed circular cylindrical shells was also tackled by Amabili, Pellicano, and Vakakis [5, 28]. In that case, only one of the low-frequency modes was excited, and solutions to a particular case for the parameter values was analytically and numerically exhibited. Finally, a 1:2:4 resonance has been studied by Nayfeh et al. [25], where the excitation frequency was selected in the vicinity of the high-frequency mode.

Our interest is also directed toward the modeling of musical instruments, where the tuning of eigenfrequencies is generally searched for, as this property sounds better to the ears. Secondly, the particular

sound of some musical instruments can be explained by some nonlinearities, such that they appear as a case where nonlinear resonances between numerous eigenfrequencies should be key to properly understand their dynamical behavior. The string is obviously the most common case for string instruments sharing the two properties of nonlinear vibrations together with commensurable eigenfrequencies; see, e.g., [12, 17, 18, 32]. Nonlinearities are also encountered in reed instruments such as saxophone and clarinette; see, e.g., [27] and brass instruments (see, e.g., [20]) and references therein. For percussion instruments, gongs, cymbals, and steelpans (or steeldrums) are also known for displaying geometric nonlinearity due to the large amplitude vibrations of the main shell structure. In the case of gongs and cymbals, internal resonances between eigenfrequencies are known to make easier the transition to chaos (or wave turbulence) that explains their particular shimming sound [7, 37]. For steelpans, the eigenfrequencies are intentionally tuned to give rise to nonlinear exchanges of energy between those modes that explains the particular timbre of the instrument [1–4]. The analytical results presented in this contribution are driven by the common occurrence of 1:2:2 and 1:2:4 resonances in numerous instruments of the steelpan family [19].

This contribution is thus focused on two internal resonances involving quadratic nonlinearity, as well as the presence of three modes: the 1:2:4 case, where the eigenfrequencies ( $\omega_1, \omega_2, \omega_3$ ) of the system are such that  $\omega_3 \simeq 2\omega_2 \simeq 4\omega_1$ , and the 1:2:2 case where  $\omega_3 \simeq \omega_2 \simeq 2\omega_1$ . The two cases have been grouped together so as to highlight the analogies and differences between them and the more classical 1:2 resonance. The aim of the present paper is also to fill the gap between already published result so as to present them in a unified manner. Although has already been studied in [25], the excitation frequency was in the vicinity of the third mode only. Here, the results are complemented by taking into account an excitation frequency in the vicinity of the first two modes. The results are generalized and thorough parametric studies in each case allow one to get a complete picture of the dynamical solutions. For the 1:2:2 case, our results also complement those of Lee and Perkins [16] by considering all possible excitation frequencies. We also consider the case where both high-frequency modes are excited simultaneously, which renders the analysis more complex as the fundamental solution involves two directly excited modes. The starting point of this study

is the general equations (under their normal form) of the considered resonances in order to obtain results that are not restricted to the particular case of a given structure but which can be applied to any system. Parametric study with important parameters of the problem (detuning parameters, damping ratios, nonlinear coupling coefficients) is also reported for the two cases. Only primary resonances are considered, which means that the case of sub or superharmonic excitations is not reported.

## 2 The 1:2:4 resonance

This section is devoted to the analysis of a system exhibiting a one-two-four (1:2:4) internal resonance, corresponding to the interaction between three vibration modes with frequencies  $\omega_1, \omega_2, \omega_3$ , such that  $\omega_2 \simeq 2\omega_1$  and  $\omega_3 \simeq 4\omega_1$ . Harmonically forced vibrations are considered, and the three cases of a forcing frequency  $\Omega$  being in the vicinity of (i) the high-frequency  $\Omega \approx \omega_3$ , (ii) the mid-frequency  $\Omega \approx \omega_2$ , and (iii) the low-frequency  $\Omega \approx \omega_1$ , are studied.

### 2.1 Equations of motion and multiple scales solution

The dynamical system for the 1:2:4 internal resonance consists of three oscillator equations coupled by quadratic nonlinear terms. It reads:

$$\ddot{q}_1 + \omega_1^2 q_1 = \varepsilon [\alpha_1 q_1 q_2 - 2\mu_1 \dot{q}_1 + \delta_{\Omega, \omega_1} F_1 \cos \Omega t], \quad (1a)$$

$$\begin{aligned} \ddot{q}_2 + \omega_2^2 q_2 \\ = \varepsilon [\alpha_2 q_1^2 + \alpha_3 q_2 q_3 - 2\mu_2 \dot{q}_2 + \delta_{\Omega, \omega_2} F_2 \cos \Omega t], \end{aligned} \quad (1b)$$

$$\ddot{q}_3 + \omega_3^2 q_3 = \varepsilon [\alpha_4 q_2^2 - 2\mu_3 \dot{q}_3 + \delta_{\Omega, \omega_3} F_3 \cos \Omega t]. \quad (1c)$$

According to perturbation methods, nonlinear terms (parameterized by  $\alpha_{1,2,3,4}$ ), damping terms (modal damping is assumed via  $\mu_{1,2,3}$ ) and external forcing ( $F_k \cos \Omega t$  with  $\delta_{\Omega, \omega_k}$  the Kronecker delta symbol used to distinguish the forced cases) are assumed to be small as compared to the linear oscillatory part, and thus are scaled by a bookkeeping device  $\varepsilon \ll 1$ .

Only four nonlinear quadratic terms are present. They correspond to the resonant monoms, and Eqs. (1a)–(1c) is the normal form of the 1:2:4 internal

resonance [6, 13, 31, 38]. All other possible nonlinear (quadratic) terms have no importance for the global dynamics and can be canceled by a nonlinear change of coordinates. Equivalently, deriving a first-order perturbation scheme with other terms (e.g.,  $q_1^2$  on (1a)), one would find that these terms do not appear in the solvability condition.

In order to express the internal resonance relationships, two internal detuning parameters  $\sigma_1$  and  $\sigma_2$  are introduced as

$$\omega_2 = 2\omega_1 + \varepsilon \sigma_1, \quad (2a)$$

$$\omega_3 = 2\omega_2 + \varepsilon \sigma_2 = 4\omega_1 + \varepsilon (2\sigma_1 + \sigma_2). \quad (2b)$$

Finally,  $\sigma$  is the external detuning, expressing the fact that the excitation frequency is selected in the vicinity of one eigenfrequency  $\omega_k$ , with  $k = 1, 2$ , or 3:

$$\Omega = \omega_k + \varepsilon \sigma. \quad (3)$$

System (1a)–(1c) is solved by the multiple scales method, using several time scales ( $T_j = \varepsilon^j t$ ), to the first order as

$$q_k(t) = q_{k0}(T_0, T_1) + \varepsilon q_{k1}(T_0, T_1) + o(\varepsilon^2), \quad (4)$$

where  $T_0 = t$  is a fast time scale and  $T_1 = \varepsilon t$  is a slow time scale.

The  $\varepsilon^0$ -order equations lead to express the  $\{q_{k0}\}_{k=1,2,3}$  as

$$q_{k0}(T_0, T_1) = \frac{a_k(T_1)}{2} \exp[j(\omega_k T_0 + \theta_k(T_1))] + \text{c.c.}, \quad (5)$$

where  $a_k$  are the amplitudes,  $\theta_k$  are the phases, c.c. stands for complex conjugate and  $j^2 = -1$ .

Introducing (5) into the  $\varepsilon^1$ -order equations leads to the so-called solvability condition, which can be written as a six-dimensional dynamical system by separating real and imaginary parts:

$$\begin{aligned} a_1' = -\mu_1 a_1 + \frac{\alpha_1 a_1 a_2}{4\omega_1} \sin(\sigma_1 T_1 + \theta_2 - 2\theta_1) \\ + \delta_{\Omega, \omega_1} \frac{F_1}{2\omega_1} \sin(\sigma T_1 - \theta_1), \end{aligned} \quad (6a)$$

$$\begin{aligned} a_1 \theta_1' = -\frac{\alpha_1 a_1 a_2}{4\omega_1} \cos(\sigma_1 T_1 + \theta_2 - 2\theta_1) \\ - \delta_{\Omega, \omega_1} \frac{F_1}{2\omega_1} \cos(\sigma T_1 - \theta_1), \end{aligned} \quad (6b)$$

$$\begin{aligned}
a_2' = & -\mu_2 a_2 - \frac{\alpha_2 a_1^2}{4\omega_2} \sin(\sigma_1 T_1 + \theta_2 - 2\theta_1) \\
& + \frac{\alpha_3 a_2 a_3}{4\omega_2} \sin(\sigma_2 T_1 + \theta_3 - 2\theta_2) \\
& + \delta_{\Omega, \omega_2} \frac{F_2}{2\omega_2} \sin(\sigma T_1 - \theta_2), \quad (6c)
\end{aligned}$$

$$\begin{aligned}
a_2 \theta_2' = & -\frac{\alpha_2 a_1^2}{4\omega_2} \cos(\sigma_1 T_1 + \theta_2 - 2\theta_1) \\
& - \frac{\alpha_3 a_2 a_3}{4\omega_2} \cos(\sigma_2 T_1 + \theta_3 - 2\theta_2) \\
& - \delta_{\Omega, \omega_2} \frac{F_2}{2\omega_2} \cos(\sigma T_1 - \theta_2), \quad (6d)
\end{aligned}$$

$$\begin{aligned}
a_3' = & -\mu_3 a_3 - \frac{\alpha_4 a_2^2}{4\omega_3} \sin(\sigma_2 T_1 + \theta_3 - 2\theta_2) \\
& + \delta_{\Omega, \omega_3} \frac{F_3}{2\omega_3} \sin(\sigma T_1 - \theta_3), \quad (6e)
\end{aligned}$$

$$\begin{aligned}
a_3 \theta_3' = & -\frac{\alpha_4 a_2^2}{4\omega_3} \cos(\sigma_2 T_1 + \theta_3 - 2\theta_2) \\
& - \delta_{\Omega, \omega_3} \frac{F_3}{2\omega_3} \cos(\sigma T_1 - \theta_3), \quad (6f)
\end{aligned}$$

where  $(\cdot)'$  stands for the derivation with respect to  $T_1$ .

Then the following variables allow the definition of an autonomous dynamical system:

$$\begin{aligned}
\gamma &= \sigma T_1 - \theta_k, & \gamma_1 &= \sigma_1 T_1 + \theta_2 - 2\theta_1, \\
\gamma_2 &= \sigma_2 T_1 + \theta_3 - 2\theta_2, \quad (7)
\end{aligned}$$

with  $k = 1, 2, 3$  depending on the excited mode.

Introducing Eqs. (7) into the dynamical system (6a)–(6f), one can obtain the fixed points giving the oscillatory solutions of this initial dynamical system. They are exhibited in the next subsections for the three different cases of excitation frequency.

## 2.2 High-frequency excitation

We begin with the case where the third oscillator, having the highest frequency  $\omega_3$ , is directly driven at its resonance. Although this case has been analyzed by Nayfeh et al. [25], it is here reconsidered. Firstly, in order to point out the similarities between this case and the two other forcing cases ( $\Omega \approx \omega_2$ , Sect. 2.3 and  $\Omega \approx \omega_1$ , Sect. 2.4), which were not considered in [25]. Secondly, it enables to highlight how the 1:2 internal resonance case allows a global understanding of the

1:2:4 case as a cascade of two 1:2 resonances. Thirdly, a thorough parametric study of the behavior of the solution branches with respect to the physical parameters is here provided with a focus on the instability of the fully coupled case, whereas Nayfeh et al. were more interested in the transition to chaos in [25].

The external detuning is introduced with

$$\Omega = \omega_3 + \varepsilon \sigma. \quad (8)$$

According to Eqs. (5) and (7), in this high-frequency case, the  $\varepsilon^0$ -order solutions leads to the third directly excited mode, oscillating at the frequency  $\Omega \simeq \omega_3$ , and the appearance of two subharmonic resonant responses for the two other modes, oscillating at  $\Omega/2$  and  $\Omega/4$  as

$$q_1(t) = a_1 \cos\left(\frac{\Omega}{4}t + \phi_1\right), \quad (9a)$$

$$q_2(t) = a_2 \cos\left(\frac{\Omega}{2}t + \phi_2\right), \quad (9b)$$

$$q_3(t) = a_3 \cos(\Omega t + \phi_3), \quad (9c)$$

where  $\phi_1 = -(\gamma + \gamma_2 + 2\gamma_1)/4$ ,  $\phi_2 = -(\gamma + \gamma_2)/2$  and  $\phi_3 = -\gamma$ .

The fixed points of (6a)–(6f) for the high-frequency excitation are found by replacing  $(\theta_1, \theta_2, \theta_3)$  by  $(\gamma, \gamma_1, \gamma_2)$ , according to Eqs. (7), and then by canceling the time derivatives ( $a_1' = \gamma_1' = a_2' = \gamma_2' = a_3' = \gamma' = 0$ ), leading to:

$$-\mu_1 a_1 + \frac{\alpha_1 a_1 a_2}{4\omega_1} \sin(\gamma_1) = 0, \quad (10a)$$

$$\begin{aligned}
\sigma_1 - \frac{\alpha_2 a_1^2}{4\omega_2 a_2} \cos(\gamma_1) - \frac{\alpha_3 a_3}{4\omega_2} \cos(\gamma_2) \\
+ \frac{\alpha_1 a_2}{2\omega_1} \cos(\gamma_1) = 0, \quad (10b)
\end{aligned}$$

$$-\mu_2 a_2 - \frac{\alpha_2 a_1^2}{4\omega_2} \sin(\gamma_1) + \frac{\alpha_3 a_2 a_3}{4\omega_2} \sin(\gamma_2) = 0, \quad (10c)$$

$$\begin{aligned}
\sigma_2 - \frac{\alpha_4 a_2^2}{4\omega_3 a_3} \cos(\gamma_2) + \frac{\alpha_2 a_1^2}{2\omega_2 a_2} \cos(\gamma_1) + \frac{\alpha_3 a_3}{2\omega_2} \cos(\gamma_2) \\
- \frac{F_3}{2\omega_3 a_3} \cos(\gamma) = 0, \quad (10d)
\end{aligned}$$

$$-\mu_3 a_3 - \frac{\alpha_4 a_2^2}{4\omega_3} \sin(\gamma_2) + \frac{F_3}{2\omega_3} \sin(\gamma) = 0, \quad (10e)$$

$$\sigma + \frac{\alpha_4 a_2^2}{4\omega_3 a_3} \cos(\gamma_2) + \frac{F_3}{2\omega_3 a_3} \cos(\gamma) = 0. \quad (10f)$$

From Eqs. (10a)–(10f), one can show that only three kinds of solutions are possible:

- (i) The *single-degree-of-freedom solution* (sdof), corresponding to  $a_3 \neq 0$ ;  $a_1 = a_2 = 0$ . In this case, only the directly excited mode participates to the vibration, without any transfer of energy neither to  $a_2$  nor to  $a_1$ .
- (ii) The *partially coupled solution* (c1) where  $a_1 = 0$ ,  $a_2 \neq 0$  and  $a_3 \neq 0$ . In this case, the two upper modes are coupled while the first one stays at rest. It can be noticed that a partially coupled solution with  $a_1 \neq 0$ ,  $a_2 = 0$ , and  $a_3 \neq 0$  is not possible, since imposing  $a_2 = 0$  in (12a) leads to  $a_1 = 0$ .
- (iii) The *fully coupled solution* (c2) where  $a_1 \neq 0$ ,  $a_2 \neq 0$  and  $a_3 \neq 0$ . The three modes are now coupled and energy has been transferred from  $a_3$  to  $a_2$  and  $a_1$ .

We now investigate the behavior and stability of the three possible solutions sdof, c1, and c2.

### 2.2.1 Single-mode solution

From the system (10a)–(10f) simplified with  $a_1 = a_2 = 0$ , the single degree-of-freedom solution is obtained as

$$a_3^{\text{sdof}} = \frac{F_3}{2\omega_3 \sqrt{\sigma^2 + \mu_3^2}}. \quad (11)$$

It corresponds to the classical resonant solution for linear oscillator with external forcing, displaying a maximum response  $a_{3\text{max}}^{\text{sdof}} = \frac{F_3}{2\omega_3 \mu_3}$  when  $\sigma = 0$ .

The stability analysis is performed by computing the Jacobian matrix of the fixed points system (10a)–(10f) along the sdof solution (i.e., by setting  $a_1 = a_2 = 0$ ), which reads

$$\mathcal{J} = \begin{pmatrix} -\mu_1 & 0 & 0 & 0 & 0 & 0 & 0 \\ 0 & 0 & \frac{\alpha_1}{2\omega_1} \cos(\gamma_1) & \frac{\alpha_3 a_3}{4\omega_2} \sin(\gamma_2) & -\frac{\alpha_3}{4\omega_2} \cos(\gamma_2) & 0 & 0 \\ 0 & 0 & -\mu_2 + \frac{\alpha_3 a_3}{4\omega_2} \sin(\gamma_2) & 0 & 0 & 0 & 0 \\ 0 & 0 & 0 & -\frac{\alpha_3 a_3}{2\omega_2} \sin(\gamma_2) & \frac{\alpha_3}{2\omega_2} \cos(\gamma_2) + \frac{F_3}{2\omega_3 a_3^2} \cos(\gamma) & \frac{F_3}{2\omega_3 a_3} \sin(\gamma) & 0 \\ 0 & 0 & 0 & 0 & -\mu_3 & \frac{F_3}{2\omega_3} \cos(\gamma) & 0 \\ 0 & 0 & 0 & 0 & -\frac{F_3}{2\omega_3 a_3^2} \cos(\gamma) & -\frac{F_3}{2\omega_3 a_3} \sin(\gamma) & 0 \end{pmatrix}.$$

The corresponding eigenvalues are

$$\lambda_1^{\text{sdof}} = 0, \quad (12a)$$

$$\lambda_2^{\text{sdof}} = -\mu_1, \quad (12b)$$

$$\lambda_3^{\text{sdof}} = -\frac{\alpha_3 a_3}{2\omega_2} \sin(\gamma_2), \quad (12c)$$

$$\lambda_4^{\text{sdof}} = -\mu_2 + \frac{\alpha_3 a_3}{4\omega_2} \sin(\gamma_2), \quad (12d)$$

$$\lambda_{5,6}^{\text{sdof}} = -\mu_3 \pm i\sigma. \quad (12e)$$

If all real parts are negative, the corresponding fixed point is stable, otherwise it is unstable. The two last eigenvalues  $\lambda_{5,6}^{\text{sdof}}$  correspond to the stability of the sdof solution with respect to perturbations along  $(a_3, \gamma)$ , i.e., the third, directly excited, oscillator. They have thus a negative real part since a single dof linear damped oscillator is stable. The first two eigenvalues

describe the perturbations brought by the first oscillator. As no direct coupling between oscillators 1 and 3 exists (solutions of the type  $a_2 = 0$ ,  $a_1 \neq 0$ ,  $a_3 \neq 0$  are not possible), they indicate stability and marginality. Finally, only one pair of eigenvalues  $\lambda_{3,4}^{\text{sdof}}$  is responsible for the stability of the sdof solution with respect to the perturbations brought by the existence of the second oscillator. The stability can thus be derived from the sign of the product  $\lambda_3 \lambda_4$ , and by determining the angle  $\sin(\gamma_2)$  thanks to Eqs. (10d) and (10f). Finally, the following stability condition for the sdof solution is obtained as:

$$a_3^{\text{sdof}} \leq I_a, \quad \text{where } I_a = \frac{2\omega_2}{\alpha_3} \sqrt{4\mu_2^2 + (\sigma_2 + \sigma)^2}. \quad (13)$$

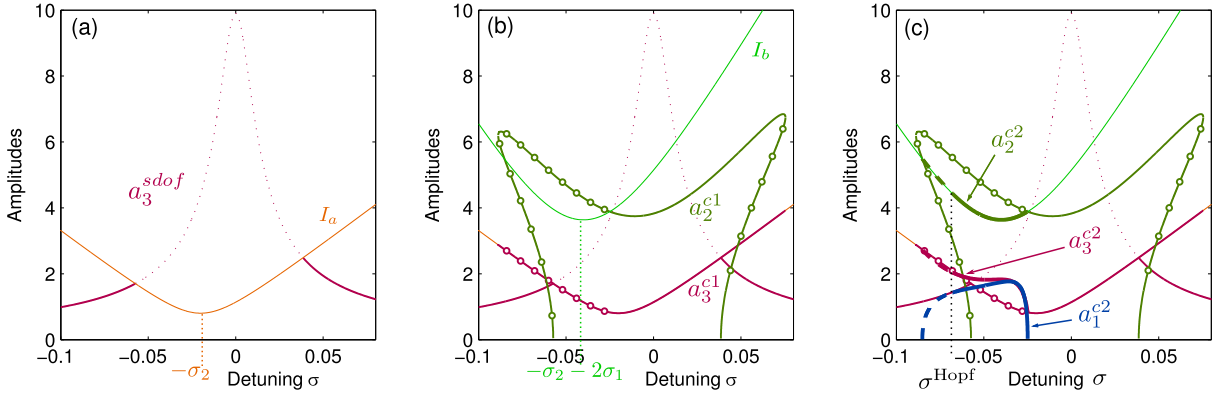


**Fig. 1** Frequency-response curves of the 1:2:4 internal resonance for a high-frequency excitation case ( $\Omega = \omega_3 + \sigma$ ). Stability behavior of the three kind of solutions: ( $\cdot \cdot \cdot$ ) sdof unstable solution, ( $- \circ -$ ) c1 unstable solution, and ( $- -$ ) c2 unstable solution. (a) Sdof solution and instability limit defined

This stability condition is reported in Fig. 1(a), where the sdof solution is also represented. Once the amplitude  $a_3$  is larger than  $I_a$ , the sdof solution becomes unstable. One can notice that this first instability is completely equivalent to a simple 1:2 internal resonance where the higher mode is excited; see, e.g., [23, 24, 33]. The instability region is fully characterized by its minimum value:

$$\text{for } \sigma = -\sigma_2, \quad I_{a,\min} = \frac{4\omega_2\mu_2}{\alpha_3}, \quad (14)$$

as well as by the slope of its asymptotic values

$$\text{for } |\sigma| \rightarrow \infty, \quad I_a \approx \frac{2\omega_2\sigma}{\alpha_3}. \quad (15)$$

In particular, these two relationships show that increasing  $\alpha_3$ , and/or decreasing  $\mu_2$ , favor the instability of the sdof solution.

It can be noticed that the two asymptotes are deduced by canceling  $\mu_2$  in  $I_a$ , that leads to  $I_a = \pm 2\omega_2(\sigma_2 + \sigma)/\alpha_3$  (see Eq. (13)). The intersection of these two curves is obtained for  $\sigma = -\sigma_2$  that is equivalent to  $\Omega = \omega_3 - \varepsilon\sigma_2 = 2\omega_2$ .

### 2.2.2 c1 solution: partially coupled 2:4 solution

When  $a_3^{\text{sdof}}$  becomes unstable, the energy injected into the system can be transferred to the second oscillator thanks to the nonlinear coefficient  $\alpha_4$  (Eqs. (1a)–(1c)).

by  $I_a$ . (b) Partially coupled 2:4 solution (c1) with its instability limit defined by  $I_b$ . (c) Fully coupled 1:2:4 solution (c2) with its Hopf bifurcation occurring at  $\sigma^{\text{Hopf}} = -0.07$ . Selected values:  $\omega_1 = 1$ ,  $\omega_2 = 2.01$ ,  $\omega_3 = 4.04$ ,  $\mu_1 = 0.01$ ,  $\mu_2 = 0.01$ ,  $\mu_3 = 0.01$ ,  $\alpha_1 = 0.011$ ,  $\alpha_2 = 0.1$ ,  $\alpha_3 = 0.1$ ;  $\alpha_4 = 0.1$ ,  $F_3 = 0.8$

The partially coupled solution is deduced from the system (10a)–(10f), simplified with  $a_1 = 0$ . Two new solutions for the amplitudes  $a_3^{c1}$  and  $a_2^{c1}$  are obtained:

$$(a_2^{c1})^2 = \frac{16\omega_2\omega_3}{\alpha_3\alpha_4} \left( -(\mu_2\mu_3 - v_2v_3) + \sqrt{\left( \frac{F_3\alpha_3}{8\omega_2\omega_3} \right)^2 - (v_2\mu_3 + \mu_2v_3)^2} \right), \quad (16)$$

$$a_3^{c1} = \frac{4\omega_2}{\alpha_3} \sqrt{\mu_2^2 + v_2^2},$$

where  $v_2 = \frac{(\sigma + \sigma_2)}{2}$  and  $v_3 = \sigma$ .

Once again, this coupled solution is equivalent to that found for two oscillators presenting a 1:2 internal resonance, except that here the coupling is between oscillators 2 and 3, so that this case may also be called the partially coupled 2:4 solution. The stability of this solution with respect to the presence of the first oscillator is now deduced from the Jacobian of the system (10a)–(10f) with  $a_1 = 0$ ,  $a_2 = a_2^{c1}$ , and  $a_3 = a_3^{c1}$ . The Jacobian is fully separable. It can be analyzed in an equivalent manner to the previous discussion in Sect. 2.2.1.

Within the six eigenvalues, only the first two dictates the stability of the c1 solution with respect to the fully coupled case where energy is shared between the



three oscillators. They read

$$\lambda_1^{c1} = -\mu_1 + \frac{\alpha_1 a_2^{c1}}{4\omega_1} \sin(\gamma_1), \quad (17a)$$

$$\lambda_2^{c1} = -\frac{\alpha_1 a_2^{c1}}{2\omega_1} \sin(\gamma_1). \quad (17b)$$

Interestingly, these two eigenvalues depend only on  $a_2^{c1}$  and not on  $a_3^{c1}$ , so that a simple stability criterion can be derived as in the previous case, by inspecting the sign of the product  $\lambda_1^{c1} \lambda_2^{c1}$ , which gives

$$a_2^{c1} \leq I_b, \quad \text{where } I_b = \frac{2\omega_1}{\alpha_1} \sqrt{4\mu_1^2 + \left(\frac{\sigma + \sigma_2 + 2\sigma_1}{2}\right)^2}. \quad (18)$$

Hence, the stability of the c1 solution is only determined by the values of  $a_2^{c1}$  with a stability limit  $I_b$  having an expression similar to  $I_a$ . In the same manner, one can deduce the minimum value of  $I_b$ :

$$\text{for } \sigma = -\sigma_2 - 2\sigma_1, \quad I_{b,\min} = \frac{4\omega_1 \mu_1}{\alpha_1}, \quad (19)$$

as well as its asymptotic behavior for large values of  $\sigma$ :

$$\text{for } |\sigma| \rightarrow \infty, \quad I_b \approx \frac{2\omega_1 \sigma}{\alpha_1}. \quad (20)$$

As in the previous case, the asymptotes are obtained by canceling  $\mu_1$  in  $I_b$  Eq. (18), with the intersection at  $\sigma = -\sigma_2 - 2\sigma_1$  that is  $\Omega = \omega_3 - \varepsilon(\sigma_2 + 2\sigma_1) = 4\omega_1$ .

These expressions show how the detuning parameter  $(\sigma_2 + 2\sigma_1)$ , the coupling coefficient  $\alpha_1$ , and the damping  $\mu_1$ , influence the stability of the c1 solution and the possibility to obtain a fully coupled solution. The stability curve  $I_b$  is represented in Fig. 1(b), for selected values of the parameters. One can remark that for the c1 solution,  $a_3^{c1}$  takes exactly the value of the stability region  $I_a$ , so that the two curves are the same. For a certain detuning  $\sigma$ , the value of  $a_2$  becomes larger than  $I_b$ . At that point, the c1 solution becomes unstable in favor of a fully coupled solution. Finally, one must be aware that the four other eigenvalues that have not been inspected here, may also have positive real parts for certain parameter values. This case is not explicated here as it can be easily recovered from known results on the 1:2 internal resonance [23, 24].

### 2.2.3 c2 solution: fully coupled 1:2:4 solution

From the fixed-points equations (10a)–(10f) and without canceling any amplitude, one can derive the solution for the c2 case. A simple expression is found for  $a_2$  as

$$a_2^{c2} = \frac{4\omega_1}{\alpha_1} \sqrt{v_1^2 + \mu_1^2}, \quad \text{where } v_1 = \frac{(\sigma + \sigma_2 + 2\sigma_1)}{4}. \quad (21a)$$

Defining

$$\chi_1(a_2^{c2}) = \frac{16\omega_1\omega_2}{\alpha_1\alpha_2}(\mu_1\mu_2 - v_1v_2) + \frac{\alpha_4\alpha_3}{\alpha_1\alpha_2} \frac{\omega_1}{\omega_3} \frac{\mu_1\mu_3 + v_1v_3}{(\mu_3^2 + v_3^2)} (a_2^{c2})^2, \quad (21b)$$

$$\chi_2(a_2^{c2}) = \frac{16\omega_2^2}{\alpha_2^2} (\mu_2^2 + v_2^2) (a_2^{c2})^2 - \frac{1}{(\mu_3^2 + v_3^2)} \times \left[ \frac{\alpha_3^2 F_3^2}{4\omega_3^2 \alpha_2^2} - \frac{2\alpha_4\alpha_3\omega_2}{\alpha_2^2 \omega_3} (\mu_2\mu_3 - v_2v_3) \right] \times (a_2^{c2})^2 - \frac{\alpha_4^2 \alpha_3^2}{16\omega_3^2 \alpha_2^2} (a_2^{c2})^4 \Big] (a_2^{c2})^2, \quad (21c)$$

one obtains, for  $a_1$  and  $a_3$ :

$$a_1^{c2} = \sqrt{-\chi_1(a_2^{c2}) + \sqrt{\chi_1^2(a_2^{c2}) - \chi_2(a_2^{c2})}}, \quad (21d)$$

$$a_3^{c2} = \frac{1}{\sqrt{\mu_3^2 + v_3^2}} \left( \frac{F_3^2}{4\omega_3^2} - \frac{2\alpha_4\alpha_2\omega_1}{\alpha_1\alpha_3\omega_3} (\mu_1\mu_3 + v_3v_1) \times (a_1^{c2})^2 - \frac{2\alpha_4\omega_2}{\alpha_3\omega_3} (\mu_2\mu_3 - v_2v_3) (a_2^{c2})^2 - \frac{\alpha_4^2}{16\omega_3^2} (a_2^{c2})^4 \right)^{1/2}. \quad (21e)$$

Once again, the value of  $a_2$ , which drives the instability from the c1 to the c2 case, now takes a value  $a_2^{c2}$  equal to  $I_b$ , in a symmetric manner as  $a_3$  for the transition from sdof to c1. The values of  $a_1^{c2}$  is slaved to the values of  $a_2^{c2}$  through the complicated functions  $\chi_1(a_2^{c2})$  and  $\chi_2(a_2^{c2})$ . Figure 1(c) shows the complete picture with all solution branches, with a c2 solution existing in the range  $\sigma \in [-0.08; -0.02]$ .

The stability of the c2 solution is given by the Jacobian of the system without any simplification and



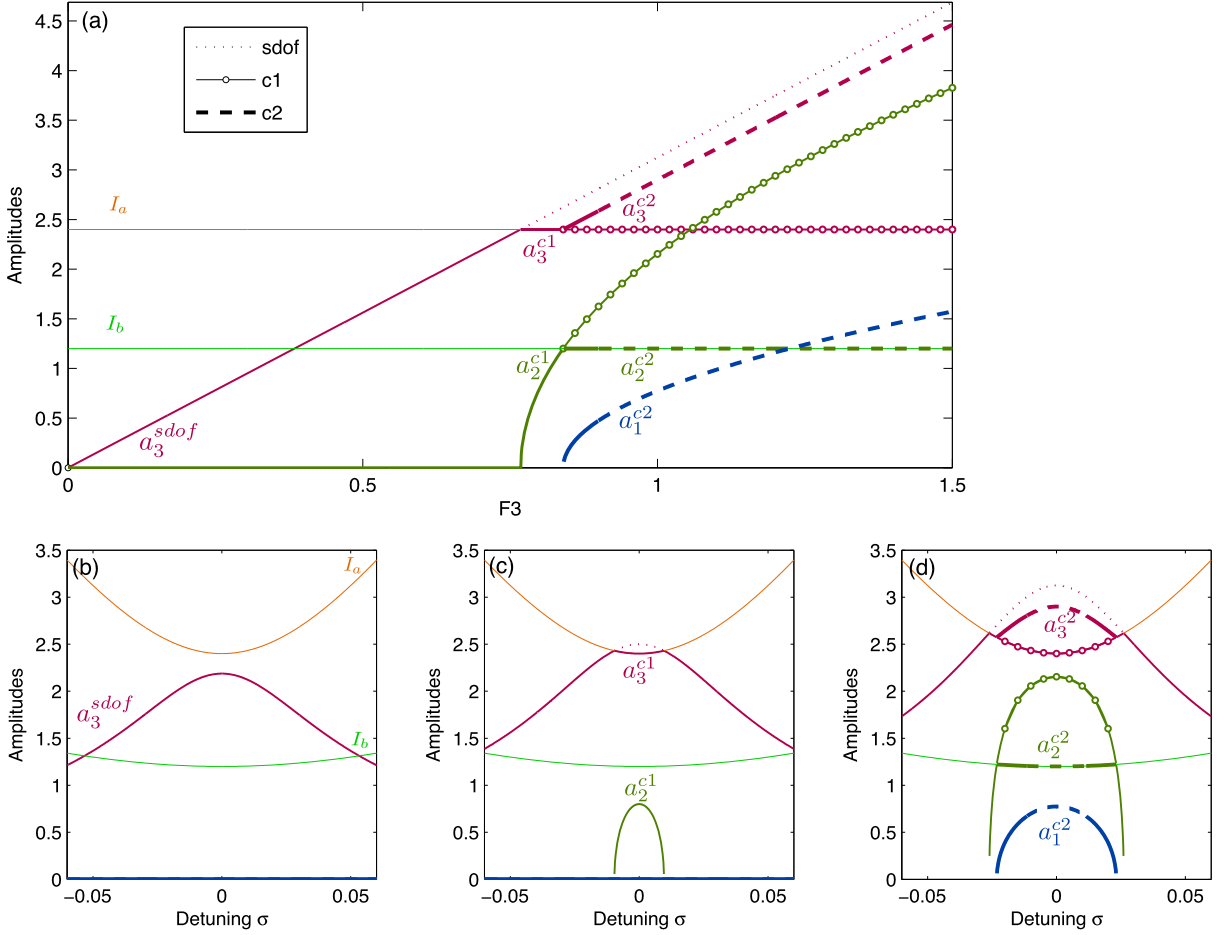


**Fig. 2** Cascade of internal resonances in the 1:2:4 internal resonance for a high-frequency excitation case ( $\Omega = \omega_3 + \sigma$ ). (a) Force-response curves. Selected values:  $\sigma = 0$ ,  $\omega_1 = 1$ ,  $\omega_2 = 2$ ,  $\omega_3 = 4$ ,  $\mu_{1,2} = 0.03$ ,  $\mu_3 = 0.04$ ,  $\alpha_{1,2,3,4} = 0.1$ . Cor-

responding frequency-response curves for  $\sigma = [-0.55 : 0.55]$  and for selected external force: (b)  $F_3 = 0.7$ , (c)  $F_3 = 0.8$ , (d)  $F_3 = 1$

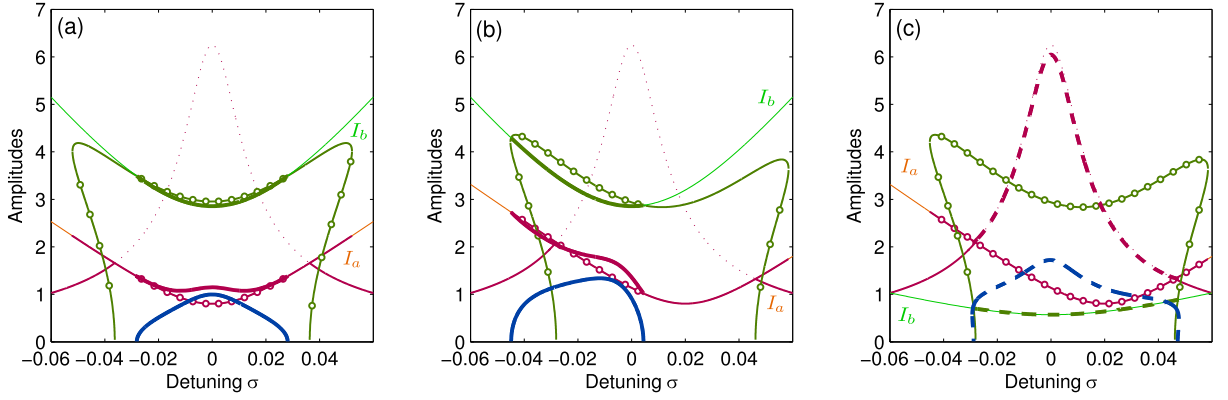
by substituting  $a_1$ ,  $a_2$ , and  $a_3$  for  $a_1^{c2}$ ,  $a_2^{c2}$ , and  $a_3^{c2}$ . In that case, no simple analytical solutions are derivable for the eigenvalues (the problem is not separable anymore), and thus the eigenvalues have to be followed numerically. In Fig. 1(c), a Hopf bifurcation has been found along the c2 branch, occurring at  $\sigma^{\text{Hopf}} = -0.07$ . At that point, no stable periodic orbits exist anymore for the oscillatory initial problem, which thus exhibit a quasiperiodic solution.

Figure 2 shows the effects of varying the excitation amplitude  $F_3$  on the response amplitude  $a_1$ ,  $a_2$  and  $a_3$ . Here, we set  $\sigma = \sigma_1 = \sigma_2 = 0$ . The figure presents the different steps of this 1:2:4 nonlinear coupling. First, for small amplitudes, only the sdof solution can exist and the system is totally stable as shown in Figs. 2(a)

and 2(b). As soon as  $a_3^{sdo}$  intersects  $I_a$ , the first coupling solutions  $a_3^{c1}$  and  $a_2^{c1}$  can appear and these new solutions are stable until  $a_2^{c1}$  intersects  $I_b$ . One can see that for  $\sigma = 0$ , when  $a_3^{c2}$  appears, the system is totally unstable and a Hopf bifurcation can exist. The dynamics presents a cascade of successive couplings that evolves here with the amplitude of the external force. Note that Fig. 2(a) shows that the c2 case is mostly unstable so that quasiperiodic solutions are more likely to occur as soon as the transfer of energy is completed.

#### 2.2.4 Parametric study

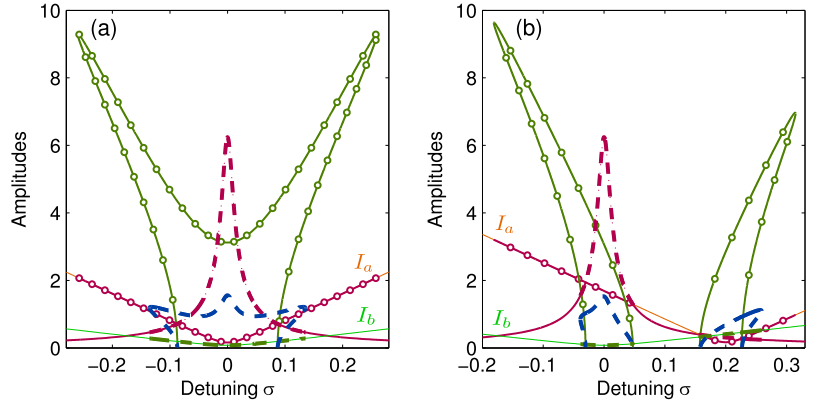
Now that the general solutions have been established, their behavior with respect to parameter variations are



**Fig. 3** Frequency-response curves of the 1:2:4 internal resonance for a high-frequency excitation case ( $\Omega = \omega_3 + \sigma$ ). (a) Stable symmetric coupled response when  $I_b > I_a$  and  $\sigma_{1,2} = 0$  (selected values:  $\omega_1 = 1$ ,  $\omega_2 = 2$ ,  $\omega_3 = 4$ ,  $\mu_{1,2,3} = 0.01$ ,  $\alpha_1 = 0.14$ ,  $\alpha_{2,3,4} = 0.1$ ,  $F_3 = 0.5$ ). (b) Stable nonsym-

metric coupled response when  $I_b > I_a$  and  $\sigma_{1,2} \neq 0$  (parameters of (a) except:  $\omega_2 = 2.01$ ). (c) Unstable nonsymmetric coupled response when  $I_a > I_b$  and  $\sigma_{1,2} \neq 0$  (parameters of (a) except:  $\omega_2 = 2.01$  and  $\alpha_1 = 0.7$ )

**Fig. 4** 1:2:4 internal resonance. Frequency-response curves when  $\Omega = \omega_3 + \sigma$ . (a)  $\omega_1 = 1$ ,  $\omega_2 = 2$ ,  $\omega_3 = 4$ ,  $\mu_1 = 0.01$ ,  $\mu_2 = 0.01$ ,  $\mu_3 = 0.01$ ,  $\alpha_{1,3} = 0.5$ ,  $\alpha_{2,4} = 0.1$ ,  $F_3 = 0.5$ . (b) Same selected values except:  $\omega_2 = 2.1$



illustrated in order to highlight the main dynamical characteristics of the 1:2:4 resonance.

Figure 3(a) shows a perfectly tuned case where  $\sigma_1 = \sigma_2 = 0$ , which leads to symmetric response with respect to the axis  $\sigma = 0$ . As noted in the previous section, the dynamics of the system excited at its higher frequency exhibits a cascade of energy from the highest (directly excited mode) to the first one, and the activation of the two steps in the cascade are completely controlled by the instability limits defined by  $a_3 < I_a$  (Eq. (13)) and  $a_2 < I_b$  (Eq. (18)). One can observe a stable 1:2:4 (c2) coupled solutions for  $\sigma \in [-0.03; 0.03]$ .

The effect of the detuning is shown in Fig. 3(b) where  $\sigma_1 = 0.01$  and  $\sigma_2 = -0.02$ . The system is not symmetric and depends on the minimum value of  $I_a$  and  $I_b$ , respectively, in  $\sigma = -\sigma_2$  and  $\sigma = -\sigma_2 - 2\sigma_1$ .

On the left part, for increasing values of  $\sigma$ , when  $a_3^{\text{sdf}}$  crosses  $I_a$ ,  $a_2$  is already unstable because of  $a_2^{c1} > I_b$  which imply that the (c2) coupled solutions are directly activated. On the contrary, for decreasing values of  $\sigma$ , the three coupling steps (sdf, c1, c2) are observed.

Figure 3(c) presents the case of the same detuning, but for a larger value of  $\alpha_1$ , implying  $I_b < I_a$ , so that only the c2 coupling can exist. One can observe that  $\alpha_1$  favors instability and leads, in that case, to a Hopf bifurcation. The c2 branch is completely unstable.

Finally, Fig. 4 shows how the branches are modified when nonlinear coupling coefficients ( $\alpha_1$  and  $\alpha_3$ ) are increased and motions of  $a_2$  and  $a_1$  go to larger amplitudes. In Fig. 4(a), a symmetric case for which  $\sigma_1 = \sigma_2 = 0$  is selected. Note also that  $I_b$  is always smaller than  $I_a$  so that the c2 solution is directly ex-

cited once the sdof solution crosses  $I_a$ . Figure 4(b) shows a more complicated behavior, which is obtained for an important detuning between the second and the third oscillator obtained here by selecting  $\omega_2 = 2.1$ . In that case,  $I_a$  crosses the sdof solution near the resonance, as well as for  $\sigma \simeq 0.2$ , far away from the linear resonance. Then, if  $I_{a,\min}$  is small enough, the coupling can be activated as shown on the figure.

As a conclusion on this high-frequency case, one can notice the important similarities with the 1:2 internal resonance case. The 1:2:4 case can be interpreted easily as a cascade of two imbricated 1:2 resonances, with two stability conditions having a similar expression. Interestingly, the fully coupled case is found to be often unstable due to a Hopf bifurcation, so that once the energy cascade to the first oscillator is achieved, quasiperiodic solutions are more likely to be observed. This can have important physical consequences, e.g., in the transition to chaotic turbulent behavior [36].

### 2.3 Mid-frequency excitation

In this section, the case where the second oscillator is directly excited is now considered. With respect to Eq. (3), the external detuning now reads

$$\Omega = \omega_2 + \varepsilon\sigma. \quad (22)$$

From Eqs. (5) and (7), the subharmonic resonant responses can be deduced as

$$q_1(t) = a_1 \cos\left(\frac{\Omega}{2}t + \phi_1\right), \quad (23a)$$

$$q_2(t) = a_2 \cos(\Omega t + \phi_2), \quad (23b)$$

$$q_3(t) = a_3 \cos(2\Omega t + \phi_3), \quad (23c)$$

where  $\phi_1 = -(\gamma + \gamma_1)/2$ ,  $\phi_2 = -\gamma$  and  $\phi_3 = \gamma_2 - 2\gamma$ .

New internal detuning parameters  $\nu_1$ ,  $\nu_2$  and  $\nu_3$  are introduced as

$$\omega_1 = \frac{1}{2}(\Omega - \varepsilon(\sigma + \sigma_1)) = \frac{\Omega}{2} - \varepsilon\nu_1, \quad (24a)$$

$$\omega_2 = \Omega - \varepsilon\sigma = \Omega - \varepsilon\nu_2, \quad (24b)$$

$$\omega_3 = 2\Omega + \varepsilon(\sigma_2 - 2\sigma) = 2\Omega + \varepsilon\nu_3, \quad (24c)$$

so that  $\nu_1 = \frac{1}{2}(\sigma + \sigma_1)$ ,  $\nu_2 = \sigma$  and  $\nu_3 = (\sigma_2 - 2\sigma)$ .

The fixed points of (6a)–(6f) for the mid-frequency case, according to Eqs. (7), are obtained as

$$-\mu_1 a_1 + \frac{\alpha_1 a_1 a_2}{4\omega_1} \sin(\gamma_1) = 0, \quad (25a)$$

$$\begin{aligned} \sigma_1 - \frac{\alpha_2 a_1^2}{4\omega_2 a_2} \cos(\gamma_1) - \frac{\alpha_3 a_3}{4\omega_2} \cos(\gamma_2) + \frac{\alpha_1 a_2}{2\omega_1} \cos(\gamma_1) \\ - \frac{F_2}{2\omega_2 a_2} \cos(\gamma) = 0, \end{aligned} \quad (25b)$$

$$\begin{aligned} -\mu_2 a_2 - \frac{\alpha_2 a_1^2}{4\omega_2} \sin(\gamma_1) + \frac{\alpha_3 a_2 a_3}{4\omega_2} \sin(\gamma_2) \\ + \frac{F_2}{2\omega_2} \sin(\gamma) = 0, \end{aligned} \quad (25c)$$

$$\begin{aligned} \sigma_2 - \frac{\alpha_4 a_2^2}{4\omega_3 a_3} \cos(\gamma_2) + \frac{\alpha_2 a_1^2}{2\omega_2 a_2} \cos(\gamma_1) + \frac{\alpha_3 a_3}{2\omega_2} \cos(\gamma_2) \\ + \frac{F_2}{\omega_2 a_2} \cos(\gamma) = 0, \end{aligned} \quad (25d)$$

$$-\mu_3 a_3 - \frac{\alpha_4 a_2^2}{4\omega_3} \sin(\gamma_2) = 0, \quad (25e)$$

$$\begin{aligned} \sigma + \frac{\alpha_2 a_1^2}{4\omega_2 a_2} \cos(\gamma_1) + \frac{\alpha_3 a_3}{4\omega_2} \cos(\gamma_2) \\ + \frac{F_2}{2\omega_2 a_2} \cos(\gamma) = 0. \end{aligned} \quad (25f)$$

Using Eqs. (25d) and (25e), one can show that letting  $a_3 = 0$  implies  $a_2 = 0$ , which is not possible since  $a_2$  is the amplitude of the directly excited mode. In fact, when the forcing is in the vicinity of the second oscillator, the system composed of oscillators 2 and 3 displays a 1:2 resonance (that will be denoted here for coherence 2:4 resonance) with the forcing on the lower frequency oscillator. It is known that only coupled solutions exist in that case [24]. Hence, only two kinds of fixed points exist for the present case:

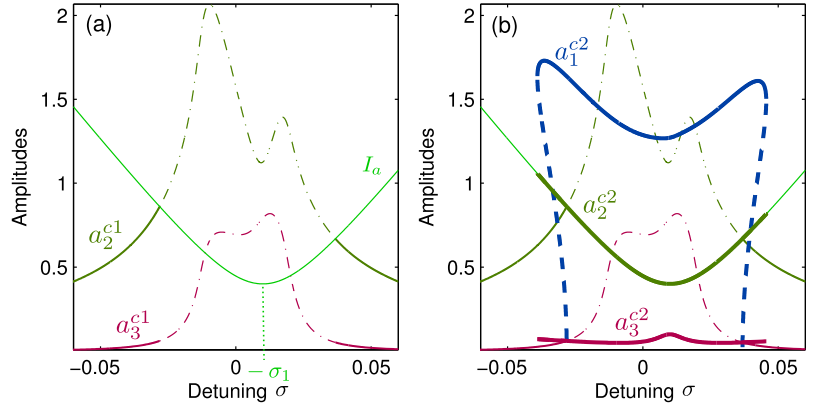
- (i) The *partially coupled solution* (c1) where  $a_1 = 0$ ,  $a_2^{c1} \neq 0$ , and  $a_3^{c1} \neq 0$ .
- (ii) The *fully coupled solution* (c2) where  $a_1^{c2} \neq 0$ ,  $a_2^{c2} \neq 0$ , and  $a_3^{c2} \neq 0$ .

The next section investigates the behavior and stability of these two types of solutions.

#### 2.3.1 c1 solution: *partially coupled 2:4 solution*

This case is equivalent to a classical 1:2 internal resonance where the excitation frequency is in the vicinity of the lowest frequency mode. Analytical solutions can be found, e.g., in [24]. They are recovered here for the

**Fig. 5** Frequency-response curves of the 1:2:4 internal resonance for a mid-frequency excitation case ( $\Omega = \omega_2 + \sigma$ ). Stability behavior of the two kind of solutions: (---) c1 unstable solution, and (- -) c2 unstable solution. Selected values:  $\omega_1 = 1$ ,  $\omega_2 = 1.99$ ,  $\omega_3 = 4$ ,  $\mu_{1,2,3} = 0.01$ ,  $\alpha_{1,2,3,4} = 0.1$ ,  $F_2 = 0.1$



2:4 resonance between oscillators 2 and 3 and read:

$$\begin{aligned} (a_2^{c1})^2 &= \frac{4\omega_3 a_3^{c1}}{\alpha_4} \sqrt{\mu_3^2 + \nu_3^2}, \\ (a_3^{c1})^3 &+ \frac{8\omega_2}{\alpha_3} \frac{(\mu_2 \mu_3 + \nu_2 \nu_3)}{\sqrt{\mu_3^2 + \nu_3^2}} (a_3^{c1})^2 + \frac{16\omega_2^2}{\alpha_3^2} \\ &\times (\mu_2^2 + \nu_2^2) a_3^{c1} - \frac{\alpha_4}{\alpha_3^2} \frac{1}{\omega_3 \sqrt{\mu_3^2 + \nu_3^2}} F_2 = 0. \end{aligned} \quad (26)$$

One can observe that  $a_3^{c1}$  is solution of a third-order polynomial. Hence, depending on the parameter values, one can obtain one or three solutions.  $a_2^{c1}$  is slaved to  $a_3^{c1}$  through a simple relationship.

The novelty in this case consists in assessing the stability of this 2:4 (c1) solution with respect to perturbations brought by the first oscillator in 1:2:4 resonance. The Jacobian matrix of system (25a)–(25f) for  $\Omega \simeq \omega_2$  and for  $a_1 = 0$  is reported in Appendix A.1. Interestingly, the six eigenvalues are separable. Four of them drive the 2 : 4 resonance and assess the usual stability conditions found for the 1:2 case [23, 24, 33]. The last two are related to the presence of the first oscillator, and writes

$$\lambda_1^{c1} = -\mu_1 + \frac{\alpha_1 a_2^{c1}}{4\omega_1} \sin(\gamma_1), \quad (27a)$$

$$\lambda_2^{c1} = -\frac{\alpha_1 a_2^{c1}}{2\omega_1} \sin(\gamma_1). \quad (27b)$$

These two eigenvalues depend only on  $a_2^{c1}$ . Hence, the stability criterion is studied by the product  $\lambda_1^{c1} \lambda_2^{c1}$ ,

which gives

$$a_2^{c1} \leq I_a \quad \text{where } I_a = \frac{2\omega_1}{\alpha_1} \sqrt{4\mu_1^2 + (\sigma + \sigma_1)^2}. \quad (28)$$

One can remark the similarity of that case with the previous one (see Sect. 2.2). Once again, the stability of the first solution is completely driven by the position of a single amplitude (here  $a_2$ ) with respect to a limit  $I_a$  having a similar expression.

As in the previous section, the stability limit  $I_a$  is characterized by its minimum value  $I_{a,\min} = \frac{4\omega_1 \mu_1}{\alpha_1}$ , obtained for  $\sigma = -\sigma_1$  as well as its asymptotic behavior for large values of  $\sigma$ , for  $|\sigma| \rightarrow \infty$ ,  $I_a \approx \frac{2\omega_1 \sigma}{\alpha_1}$ . The asymptotes are obtained with  $\mu_1 = 0$  in Eq. (28) and the intersection is found for  $\sigma = -\sigma_1$  ( $\Omega = \omega_2 - \varepsilon \sigma_1 = 2\omega_1$ ).

In this case,  $\sigma_1$ ,  $\alpha_1$ , and  $\mu_1$  are the new influential parameters on the stability curve, which is represented in Fig. 5(a) for selected parameters. The instability of the c1 solution is given by the relative values of  $a_2^{c1}$  and  $I_a$ . In the selected case, the c1 solution is unstable for  $\sigma \in [-0.028; 0.037]$ . The next subsection gives the expressions of the solution branches for case c2, when  $a_1 \neq 0$ .

### 2.3.2 c2 solution: fully coupled 1:2:4 solution

From the system (25a)–(25f) without any simplification, the fully coupled solutions are found to be:

$$a_2^{c2} = \frac{4\omega_1}{\alpha_1} \sqrt{\mu_1^2 + \nu_1^2}, \quad (29a)$$

$$a_3^{c2} = \frac{\alpha_4}{4\omega_3 \sqrt{\mu_3^2 + \nu_3^2}} (a_2^{c2})^2. \quad (29b)$$

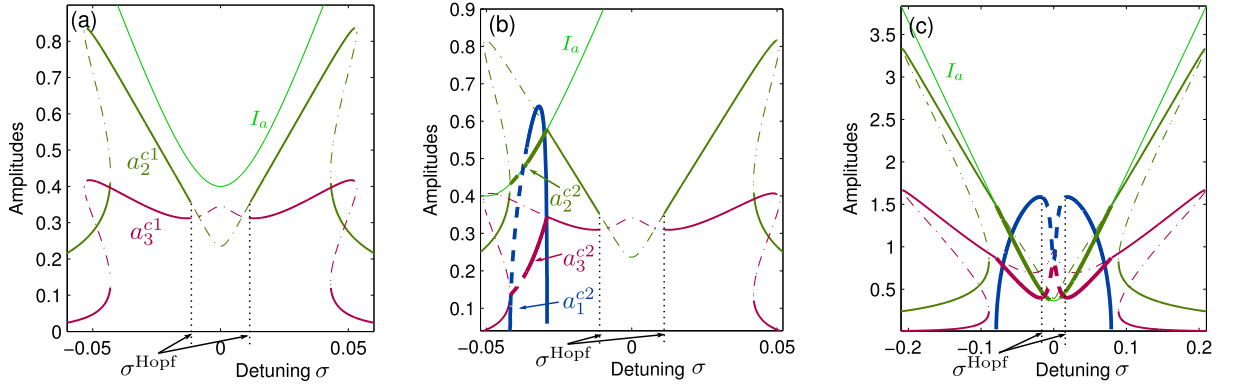


**Fig. 6** Frequency-response curves of the 1:2:4 internal resonance for a mid-frequency excitation ( $\Omega = \omega_2 + \sigma$ ). Selected values: (a) 2:4 internal coupling between  $a_2$  and  $a_3$ . Selected values:  $\omega_1 = 1$ ,  $\omega_2 = 2$ ,  $\omega_3 = 4$ ,  $\mu_{1,2,3} = 0.01$ ,  $\alpha_{1,2} = 0.1$ ,

$\alpha_{3,4} = 1$ ,  $F_2 = 0.05$ . (b) Influence of the detuning, activation of the c2 coupling. Parameters of (a) except  $\omega_2 = 2.05$ ,  $\omega_3 = 4.01$ . (c) c2 coupling in the Hopf bifurcation range. Parameters of (a) except  $\alpha_1 = 0.11$  and  $F_2 = 0.2$

Defining

$$C_4 = \left( \frac{\alpha_2}{4\omega_2 a_2^{c2}} \right)^2, \quad (29c)$$

$$C_2 = -\frac{2\omega_1 \alpha_2}{\alpha_1 \omega_2 (a_2^{c2})^2} \left[ (v_1 v_2 - \mu_1 \mu_2) + \frac{\alpha_3 \omega_3 (a_3^{c2})^2}{\alpha_4 \omega_2 (a_2^{c2})^2} (v_1 v_3 - \mu_1 \mu_3) \right], \quad (29d)$$

$$C_0 = (\mu_2^2 + v_2^2) + \frac{2\alpha_3 \omega_3 (a_3^{c2})^2}{\alpha_4 \omega_2 (a_2^{c2})^2} (\mu_2 \mu_3 + v_2 v_3) + 2 \left( \frac{\alpha_3 \omega_3 (a_3^{c2})^2}{\alpha_4 \omega_2 (a_2^{c2})^2} \right)^2 (\mu_3^2 + v_3^2) - \left( \frac{\alpha_3 a_3^{c2}}{4\omega_2} \right)^2 - \left( \frac{F_2}{2\omega_2 a_2^{c2}} \right)^2, \quad (29e)$$

$a_1^{c2}$  is given by the roots of the following equation:

$$C_4 (a_1^{c2})^4 + C_2 (a_1^{c2})^2 + C_0 = 0. \quad (29f)$$

As in the high-frequency case, the value of  $a_2$  drives the instability from the c1 to the c2 case. Once the instability of the c1 solution is obtained,  $a_2^{c2}$  is then equal to  $I_a$ . The value of  $a_3^{c2}$  is slaved to  $a_2^{c2}$ , and finally  $a_1^{c1}$  is obtained from a complicated polynomial expression, the coefficients of which depends on  $a_2^{c2}$  and  $a_3^{c2}$ .

Figure 5(b) shows the complete solutions for the mid-frequency case and the transfer of energy from the directly excited mode to the low-frequency one.

Finally, this case bears resemblance with both a 1:2 internal resonance excited at the lower frequency (through the c1 2:4 solution), and a 1:2 internal resonance excited at the highest frequency (through the instability region).

The stability of the c2 solution is obtained by the Jacobian of the system (25a)–(25f) without any simplification and with  $a_1 = a_1^{c2}$ ,  $a_2 = a_2^{c2}$ , and  $a_3 = a_3^{c2}$ . As in the previous case, the eigenvalues have to be followed numerically.

### 2.3.3 Parametric study

The main dynamical characteristics due to selected values of the parameters are now investigated.

Figure 6(a) presents a perfectly tuned symmetric case. The amplitude solutions are under the stability limit  $I_a$ , hence no energy is transferred to the low-frequency mode; consequently,  $a_1$  stays at rest. The stability computation shows the appearance of a quasiperiodic regime in the vicinity of  $\sigma = 0$ . Note that in that case, only the c2 (2:4) solution is present, so that the stability can be checked by the four eigenvalues of the 2:4 case as reported in Appendix A.1. The Hopf bifurcation in the vicinity of  $\sigma = 0$  is classical and has already been reported in studies on the 1:2 internal resonance, see e.g. [24].

In Fig. 6(b), the stability curve is shifted to the low frequencies, by detuning the three eigenfrequencies. The intersection between  $I_a$  and  $a_2$  leads to the non-linear coupling between  $a_2$  and  $a_1$ . The c1 solution is then obtained, and the stability shows that on this

fully coupled branch, a Hopf bifurcation occurs and quasiperiodic motions are at hand. This remark is consistent with the numerical results obtained in the previous section, where fully coupled periodic solutions were found to be often unstable.

Figure 6(c) exhibits a different case where the intersection between  $I_a$  and  $a_2$  is located in the center frequency range. This case is obtained for a large value of the external forcing ( $F_2 = 0.2$ ). Once again, the c2 solution is partially unstable so that quasiperiodic solutions are still present.

## 2.4 Low-frequency excitation

Finally, the case of the low-frequency excitation is presented in this subsection. The external frequency is expressed as

$$\Omega = \omega_1 + \varepsilon\sigma. \quad (30)$$

The polar forms (Eq. (5)), are now:

$$q_1(t) = a_1 \cos(\Omega t + \phi_1), \quad (31a)$$

$$q_2(t) = a_2 \cos(2\Omega t + \phi_2), \quad (31b)$$

$$q_3(t) = a_3 \cos(4\Omega t + \phi_3), \quad (31c)$$

where  $\phi_1 = -\gamma$  et  $\phi_2 = \gamma_1 - 2\gamma$  and  $\phi_3 = \gamma_2 + 2\gamma - 1 - 4\gamma$ .

The internal detunings are defined by

$$\omega_1 = \Omega - \varepsilon\sigma = \Omega - \varepsilon v_1, \quad (32a)$$

$$\omega_2 = 2\Omega + \varepsilon(\sigma_1 - 2\sigma) = 2\Omega + \varepsilon v_2, \quad (32b)$$

$$\omega_3 = 4\Omega + \varepsilon(2\sigma_1 + \sigma_2 - 4\sigma) = 4\Omega + \varepsilon v_3, \quad (32c)$$

with  $v_1 = \sigma$ ,  $v_2 = (\sigma_1 - 2\sigma)$  and  $v_3 = (\sigma_2 + 2\sigma_1 - 4\sigma)$ .

In this case, the fixed points of (6a)–(6f), according to Eqs. (7), are

$$-\mu_1 a_1 + \frac{\alpha_1 a_1 a_2}{4\omega_1} \sin(\gamma_1) + \frac{F_1}{2\omega_1} \sin(\gamma) = 0, \quad (33a)$$

$$\begin{aligned} \sigma_1 - \frac{\alpha_2 a_1^2}{4\omega_2 a_2} \cos(\gamma_1) - \frac{\alpha_3 a_3}{4\omega_2} \cos(\gamma_2) + \frac{\alpha_1 a_2}{2\omega_1} \cos(\gamma_1) \\ + \frac{F_1}{\omega_1 a_1} \cos(\gamma) = 0, \end{aligned} \quad (33b)$$

$$-\mu_2 a_2 - \frac{\alpha_2 a_1^2}{4\omega_2} \sin(\gamma_1) + \frac{\alpha_3 a_2 a_3}{4\omega_2} \sin(\gamma_2) = 0, \quad (33c)$$

$$\sigma_2 - \frac{\alpha_4 a_2^2}{4\omega_3 a_3} \cos(\gamma_2) + \frac{\alpha_2 a_1^2}{2\omega_2 a_2} \cos(\gamma_1)$$

$$+ \frac{\alpha_3 a_3}{2\omega_2} \cos(\gamma_2) = 0, \quad (33d)$$

$$-\mu_3 a_3 - \frac{\alpha_4 a_2^2}{4\omega_3} \sin(\gamma_2) = 0, \quad (33e)$$

$$\sigma + \frac{\alpha_1 a_2}{4\omega_1} \cos(\gamma_1) + \frac{F_1}{2\omega_1 a_1} \cos(\gamma) = 0. \quad (33f)$$

Equation (33a) shows that, if  $a_1 = 0$ ,  $F_1 = 0$ , which makes no sense in this excitation case. In Eq. (33c),  $a_2 = 0$  implies that  $a_1 = 0$ , which is not possible as previously said. With Eq. (33e), one can show that  $a_3 = 0$  leads to  $a_2 = 0$ . Finally, one can conclude that the only non trivial solution of system (33a)–(33f) is the fully coupled one with  $a_1 \neq 0$ ,  $a_2 \neq 0$  and  $a_3 \neq 0$ .

Some combinations of equations of the system (33a)–(33f) can exhibit analytical solutions for the three amplitudes  $a_1$ ,  $a_2$ , and  $a_3$ . First, combining Eq. (33e) with (Eq. (33f) + 2(Eq. (33d) – 2Eq. (33f))) gives a relationship between  $a_2$  and  $a_3$  as

$$a_2^2 = \frac{4\omega_3 a_3}{\alpha_4} \sqrt{(\mu_3^2 + v_3^2)}. \quad (34)$$

Then Eqs. (33a), (33b), (33c), and ((33d) – 2(33c)) gives two expressions of  $a_1$ , depending of  $a_2$  and  $a_3$

$$\begin{aligned} a_1^2(\mu_1^2 + v_1^2) \\ = \frac{F_1^2}{4\omega_1^2} - \frac{\alpha_1^2 a_1^2 a_2^2}{16\omega_1^2} - \frac{2\alpha_1 \omega_2 a_2^2}{\alpha_2 \omega_1} (v_1 v_2 + \mu_1 \mu_2) \\ + \frac{2\alpha_1 \alpha_3 \omega_3 a_3^2}{\omega_1 \alpha_2 \alpha_4} (v_1 v_3 - \mu_1 \mu_3), \end{aligned} \quad (35a)$$

$$\begin{aligned} a_1^4 = \frac{16\omega_2^2 a_2^2}{\alpha_2^2} (\mu_2^2 + v_2^2) + \frac{32\omega_2 \omega_3 \alpha_3 a_3^2}{\alpha_4 \alpha_2^2} \\ \times (\mu_2 \mu_3 - v_2 v_3) + \frac{\alpha_3^2 a_3^2 a_2^2}{\alpha_2^2}, \end{aligned} \quad (35b)$$

that leads to  $a_2^2$  given by the roots of the following five-order polynomial:

$$C_{10} a_2^{10} + C_8 a_2^8 + C_6 a_2^6 + C_4 a_2^4 + C_2 a_2^2 + C_0 = 0, \quad (36)$$

where  $C_k$  coefficients are defined and reported in Appendix A.2. Solving this polynomial for each value of  $\sigma$  gives the fully coupled solutions of this low-frequency case.

The stability of the low-frequency solutions is obtained by the Jacobian of the system (33a)–(33f) also

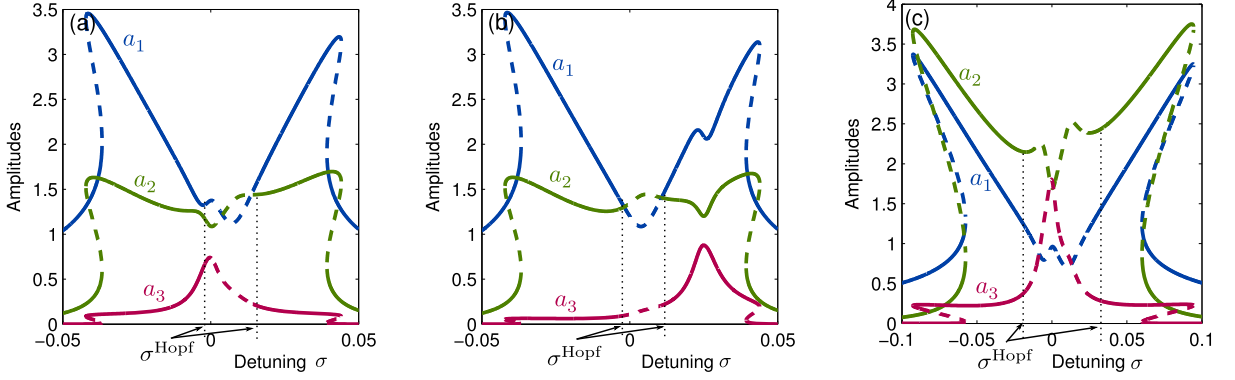


**Fig. 7** Frequency-response curves of the 1:2:4 internal resonance for a low-frequency excitation case ( $\Omega = \omega_1 + \sigma$ ). (a) Fully coupled solutions with a Hopf bifurcation, (- -) unstable solution. Selected values:  $\omega_1 = 1$ ,  $\omega_2 = 2.01$ ,  $\omega_3 = 4$ ,

$\mu_1 = 0.01$ ,  $\mu_2 = 0.01$ ,  $\mu_3 = 0.01$ ,  $\alpha_1 = 0.1$ ,  $\alpha_2 = 0.1$ ,  $\alpha_3 = 0.1$ ;  $\alpha_4 = 0.1$ ,  $F_1 = 0.1$ . (b) Detuning effects. Parameters of (a) except:  $\omega_2 = 4.1$ . (c) Parameters of (a) large amplitude of nonlinear coupling. Parameters of (a) except:  $\alpha_2 = 0.5$

reported in Appendix A.2. They are numerically calculated for each  $\sigma$  in order to obtain the stability of the solution branches.

Figure 7 displays three cases for selected values of parameters. Figure 7(a) shows a simple 1:2:4 internal resonance in the low-frequency excitation case. One can observe that the external energy, applied on the first mode is transferred to the two higher-frequency one. One can recover the behavior of a 1:2 internal resonance [24] with the hysteresis loop between forward and backward frequency sweeps in term of  $\sigma$ , due to the unstable branch; and the Hopf bifurcation leading to a quasiperiodic regime around  $\sigma = 0.01$ .

The effect of the detuning is shown Fig. 7(b) with  $\sigma_1 = 0.01$  and  $\sigma_2 = 0.08$ . One can observe that increasing the value of  $\sigma_2$  shifts the maximum value of  $a_3$  and creates corresponding variations of the amplitudes  $a_1$  and  $a_2$  at  $\sigma = 0.025$ .

Finally, Fig. 7(c) presents a case of large coupling between  $a_1$  and  $a_2$  thanks to a large value of  $\alpha_2$ , which consequently increases the range of the Hopf bifurcation for  $\sigma \in [-0.02; 0.02]$ .

## 2.5 Conclusion on the 1:2:4 resonance

In this section, a detailed analysis of the 1:2:4 internal resonance has been proposed. The study of the three excitation cases  $\Omega \simeq \omega_1$ ,  $\Omega \simeq \omega_2$ , and  $\Omega \simeq \omega_3$  are completed.

As compared to the well-known 1:2 internal resonance, each case presents some particularities due to the presence of the third oscillator.

In the high-frequency case, because of the presence of the three oscillators, two stability conditions have been found that lead to three kind of solutions (one sdof, one partially coupled, and one fully coupled). The qualitative behavior of this case is in fact a cascade of two 1:2 internal resonances. On the other hand, in the mid-frequency case, only two kinds of solutions have been found because the coupling between the mode directly excited and the high-frequency one always exists. In this case, the dynamics may be interpreted as a superposition of two internal resonances. Finally, in the low frequency case, only the fully coupled solution can exist, and the energy is always transferred to the higher modes without any stability condition.

An important result is that, in all the three cases, selected sets of parameters can cause Hopf bifurcations to occur, so that the three periodic solutions are totally unstable, giving birth to quasiperiodic regimes.

## 3 The 1:2:2 resonance

This section is devoted to the analysis of a system exhibiting a one-two-two internal resonance (1:2:2), that is another combination of two 1:2 internal resonance as compared to the previous 1:2:4 case. The interaction between three vibration modes with frequencies  $\omega_1$ ,  $\omega_2$ ,  $\omega_3$ , such that  $\omega_2 \simeq \omega_3 \simeq 2\omega_1$ , is studied. As previously, harmonically forced vibrations are considered. Two cases of a forcing frequency  $\Omega$  being in the vicinity of (i) the lower frequency  $\Omega \approx \omega_1$ , (ii) the



two higher frequencies  $\Omega \approx \omega_2 \approx \omega_3$ , are now introduced.

### 3.1 Equations of motion and multiple scales solutions

The dynamical system for the 1:2:2 internal resonance consists of three oscillator equations coupled by quadratic nonlinear terms. It reads

$$\ddot{q}_1 + \omega_1^2 q_1 = \varepsilon [-2\mu_1 \dot{q}_1 - \alpha_1 q_1 q_2 - \alpha_2 q_1 q_3 + \delta_{\Omega, \omega_1} F_1 \cos(\Omega t)], \quad (37a)$$

$$\ddot{q}_2 + \omega_2^2 q_2 = \varepsilon [-2\mu_2 \dot{q}_2 - \alpha_3 q_1^2 + \delta_{\Omega, \omega_2} F_2 \cos(\Omega t)], \quad (37b)$$

$$\ddot{q}_3 + \omega_3^2 q_3 = \varepsilon [-2\mu_3 \dot{q}_3 - \alpha_4 q_1^2 + \delta_{\Omega, \omega_2} F_3 \cos(\Omega t)]. \quad (37c)$$

As in the 1:2:4 internal resonance (Eqs. (1a)–(1c)), nonlinear terms ( $\alpha_{1,2,3,4}$ ), damping terms ( $\mu_{1,2,3}$ ) and external forcing ( $F_k \cos \Omega t$  with  $\delta_{\Omega, \omega_k}$ ) are assumed to be small as compared to the linear oscillatory part ( $\varepsilon \ll 1$ ).

Equations (37a)–(37c) is the real normal form of the system displaying 1:2:2 internal resonance. Hence, only the resonant monoms have been taken into account, so that only four coupling coefficients  $\alpha_{1,2,3,4}$  are needed to parameterize the nonlinearity, in an equivalent manner to the previous 1:2:4 case.

Two internal detuning parameters  $\sigma_1$  and  $\sigma_2$  are introduced as

$$\omega_2 = 2\omega_1 + \varepsilon \sigma_1, \quad (38a)$$

$$\omega_3 = 2\omega_1 + \varepsilon \sigma_2 \quad (38b)$$

and the external detuning  $\sigma$  is such that

$$\Omega = \omega_k + \varepsilon \sigma. \quad (39)$$

Finally, angles relationships are introduced as

$$\begin{aligned} \gamma_1 &= \theta_2 + \sigma_1 T_1 - 2\theta_1, \\ \gamma_2 &= \theta_3 + \sigma_2 T_1 - 2\theta_1, \quad \text{and} \quad \gamma = \sigma T_1 - \theta_k, \end{aligned} \quad (40)$$

where  $k = 1, 2$ , or  $3$  depending on the frequency excitation.

As in the previous section, the solvability conditions are obtained with the  $\varepsilon^0$ -order equations. The

modal amplitudes  $\{q_{k0}\}_{k=1,2,3}$  are expressed as

$$q_{k0}(T_0, T_1) = \frac{a_k(T_1)}{2} \exp[j(\omega_k T_0 + \theta_k(T_1))] + \text{c.c.}, \quad (41)$$

where  $a_k$  are the amplitudes,  $\theta_k$  are the phases, c.c. stands for complex conjugate, and  $j^2 = -1$ .

### 3.2 Low-frequency excitation

The low-frequency excitation, for which  $\Omega = \omega_1 + \varepsilon \sigma$ , is first investigated. According to Eqs. (40) and (41), the 1:2:2 internal resonance, excited on its lower mode, leads to the first mode oscillating at the frequency  $\Omega \approx \omega_1$  and the two upper modes oscillating at  $2\Omega \approx 2\omega_1$  as

$$q_1 = a_1 \cos(\Omega t + \phi_1), \quad (42a)$$

$$q_2 = a_2 \cos(2\Omega t + \phi_2), \quad (42b)$$

$$q_3 = a_3 \cos(2\Omega t + \phi_2), \quad (42c)$$

where  $\phi_1 = -\gamma$ ,  $\phi_2 = -2\gamma + \gamma_1$ , and  $\phi_3 = -2\gamma + \gamma_2$ .

The fixed points of the first-order multiple scales method are the solutions of

$$\begin{aligned} -\mu_1 a_1 - \frac{\alpha_1 a_1 a_2}{4\omega_1} \sin(\gamma_1) - \frac{\alpha_2 a_1 a_3}{4\omega_1} \sin(\gamma_2) \\ + \frac{F_1}{2\omega_1} \sin(\gamma) = 0, \end{aligned} \quad (43a)$$

$$\begin{aligned} \sigma_1 + \frac{\alpha_3 a_1^2}{4\omega_2 a_2} \cos(\gamma_1) - \frac{\alpha_1 a_2}{2\omega_1} \cos(\gamma_1) - \frac{\alpha_2 a_3}{2\omega_1} \cos(\gamma_2) \\ + \frac{F_1}{\omega_1 a_1} \cos(\gamma) = 0, \end{aligned} \quad (43b)$$

$$-\mu_2 a_2 + \frac{\alpha_3 a_1^2}{4\omega_2} \sin(\gamma_1) = 0, \quad (43c)$$

$$\begin{aligned} \sigma_2 + \frac{\alpha_4 a_1^2}{4\omega_3 a_3} \cos(\gamma_2) - \frac{\alpha_1 a_2}{2\omega_1} \cos(\gamma_1) - \frac{\alpha_2 a_3}{2\omega_1} \cos(\gamma_2) \\ + \frac{F_1}{\omega_1 a_1} \cos(\gamma) = 0, \end{aligned} \quad (43d)$$

$$-\mu_3 a_3 + \frac{\alpha_4 a_1^2}{4\omega_3} \sin(\gamma_2) = 0, \quad (43e)$$

$$\begin{aligned} \sigma - \frac{\alpha_1 a_2}{4\omega_1} \cos(\gamma_1) - \frac{\alpha_2 a_3}{4\omega_1} \cos(\gamma_2) \\ + \frac{F_1}{2\omega_1 a_1} \cos(\gamma) = 0. \end{aligned} \quad (43f)$$

From Eqs. (43a)–(43f), one can remark that only the case of fully coupled solutions are possible. Indeed,  $q_1$  is the directly excited mode so that  $a_1 \neq 0$ , and Eqs. (43c) and (43e) imply  $a_2 \neq 0$  and  $a_3 \neq 0$ . A solution in terms of the amplitudes ( $a_1, a_2, a_3$ ) of each oscillator can be found by selected linear combination of Eqs. (43a)–(43f). First, Eqs. (43d) and ((43b) – 2(43f)), and secondly Eqs. (43e) and ((43d) – 2(43f)) give a relationship between  $a_1$  and  $a_2$ , and between  $a_1$  and  $a_3$ , respectively, as

$$a_1 = \sqrt{\frac{4\omega_2 a_2}{\alpha_3 \Gamma_2}},$$

$$\text{where } \Gamma_2 = \frac{1}{\sqrt{\mu_2^2 + (\sigma_1 - 2\sigma)^2}},$$

$$a_1 = \sqrt{\frac{4\omega_3 a_3}{\alpha_4 \Gamma_3}},$$

$$\text{where } \Gamma_3 = \frac{1}{\sqrt{\mu_3^2 + (\sigma_2 - 2\sigma)^2}}.$$
(44)

This leads to a relationship between  $a_2$  and  $a_3$  as

$$a_3 = \frac{\omega_2 \alpha_4 \Gamma_3}{\omega_3 \alpha_3 \Gamma_2} a_2. \quad (45)$$

Then Eqs. (43f) and (43a) lead to

$$\begin{aligned} & \frac{4\omega_1^2}{F^2} a_1^2 \left( \sigma^2 + \mu_1^2 + \frac{\alpha_1^2}{16\omega_1^2} a_2^2 + \frac{\alpha_2^2}{16\omega_1^2} a_3^2 \right. \\ & + \frac{\alpha_1 \Gamma_2}{2\omega_1} (\mu_1 \mu_2 + \sigma(\sigma_1 - 2\sigma)) a_2 \\ & + \frac{\alpha_2 \Gamma_3}{2\omega_1} (\mu_1 \mu_3 + \sigma(\sigma_2 - 2\sigma)) a_3 \\ & + \frac{\alpha_1 \alpha_2 \Gamma_2 \Gamma_3}{8\omega_1^2} (\mu_2 \mu_3 + (\sigma_1 - 2\sigma) \\ & \left. \times (\sigma_2 - 2\sigma)) a_2 a_3 \right) = 1. \end{aligned} \quad (46)$$

Finally, introducing Eq. (45) in Eq. (46), two third-order polynomials in terms of  $a_2$  and  $a_3$  are obtained. As an example, we can write the polynomial in  $a_2$  as

$$\begin{aligned} & \left( 1 + \left( \frac{\omega_2 \alpha_2 \alpha_4 \Gamma_3}{\omega_3 \alpha_1 \alpha_3 \Gamma_2} \right)^2 + \frac{2\omega_2 \alpha_2 \alpha_4 \Gamma_3^2}{\omega_3 \alpha_1 \alpha_3} \right. \\ & \left. \times (\mu_2 \mu_3 + (\sigma_1 - 2\sigma)(\sigma_2 - 2\sigma)) \right) a_2^3 \end{aligned}$$

$$\begin{aligned} & + \left( \frac{8\omega_1 \Gamma_2}{\alpha_1} (\mu_1 \mu_2 + \sigma(\sigma_1 - 2\sigma)) \right. \\ & + \frac{8\omega_1 \omega_2 \alpha_2 \alpha_4 \Gamma_3^2}{\omega_3 \alpha_1^2 \alpha_3 \Gamma_2} (\mu_1 \mu_3 + \sigma(\sigma_2 - 2\sigma)) \left. \right) a_2^2 \\ & + \frac{16\omega_1^2}{\alpha_1^2} (\sigma^2 + \mu_1^2) a_2 = \frac{F_1^2 \alpha_3 \Gamma_2}{\omega_2 \alpha_1^2}. \end{aligned} \quad (47)$$

Hence, the amplitude solutions are deduced from Eq. (47), which shows that  $a_2$  may have one or three real solutions, depending on the parameters. Once  $a_2$  is found,  $a_1$  is deduced from Eq. (44) and  $a_3$  from Eq. (45). One can observe that Eqs. (47), (44), and (45) bear similarities with the solution equations for the 1:2 resonance case as given, e.g., in [23, 24].

The stability is given by the Jacobian derived from Eqs. (43a)–(43f). Its analytical expression is given in Appendix B.1. As no simple analytical expressions for the eigenvalues can be derived, the stability is checked numerically.

Figure 8 displays three cases with selected parameters, for small amplitude of external forcing leading to single, stable branch of solution. Only the two internal detunings  $\sigma_1$  and  $\sigma_2$  are modified. Figure 8(a) shows that the energy, which is directly injected on  $a_1$ , is simultaneously transferred to  $a_2$  and  $a_3$ . As all parameters of  $a_2$  and  $a_3$  are the same, the two corresponding curves are totally superimposed. In Fig. 8(b),  $\sigma_1 \neq \sigma_2$  which implies  $a_2 \neq a_3$ , so that the two curves are now different. Finally, in Fig. 8(c),  $\sigma_2$  is further increased, such that the maximum value is shifted to a higher frequency as compared to Fig. 8(b). Consequently, the response for  $a_1$  shows now three successive maxima, a feature that is not observable with a simple 1:2 resonance.

Larger values of the amplitude excitation  $F_1$ , leading to ranges where three solutions are possible, are investigated in Fig. 9. In Fig. 9(a), two regions where three solutions exist are present. As in the 1:2 case, the middle amplitude branch is found to be unstable. The global behavior is very similar to the 1:2 internal resonance case, with also a frequency range delimited by Hopf bifurcations where no stable periodic orbits exist anymore, so that quasiperiodic motions are at hand. A peculiarity of the 1:2:2 case is shown in Fig. 9(b). By playing with the internal detunings (here by increasing  $\sigma_2$  only), one can find in the vicinity of  $\sigma = 0$  two regions of quasiperiodic solutions, separated by a stable region (between  $\sigma = 0.0058$  and  $\sigma = 0.029$ ).

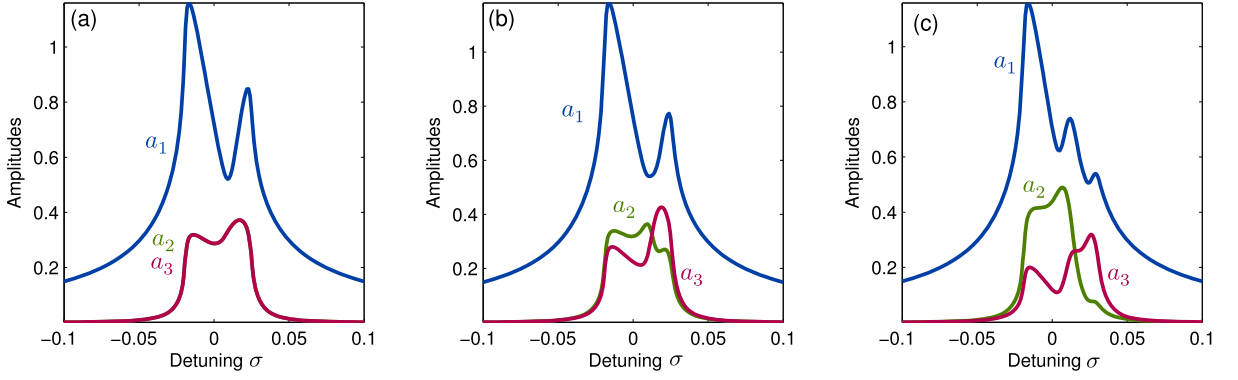
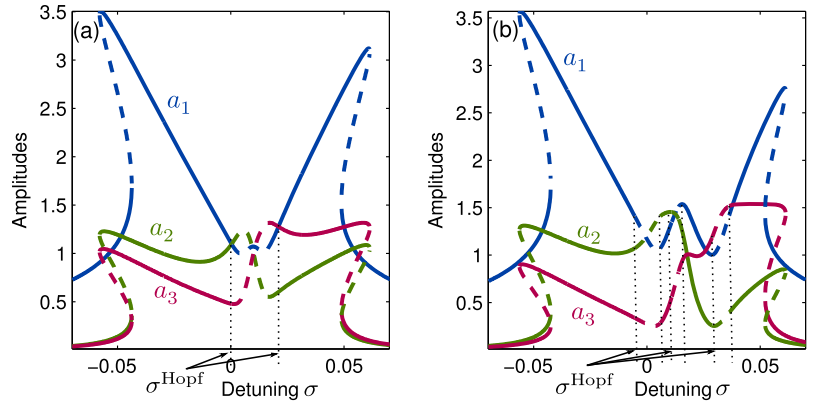


**Fig. 8** Frequency-response curves of the 1:2:2 internal resonance for a low-frequency excitation ( $\Omega = \omega_1 + \sigma$ ). Fully coupled solutions and variations of internal detunings. (a) Identical high-frequency modes. Parameters:  $\omega_1 = 1$ ,  $\omega_2 = \omega_3 = 2.02$ ,

$\mu_{1,2,3} = 0.1$ ,  $\alpha_{1,2,3,4} = 0.1$ ,  $F_1 = 0.03$ . (b) Small value of the internal detuning between  $a_2$  and  $a_3$ . Parameters of (a) except:  $\omega_3 = 2.03$ . (c) Larger value of the internal detuning between  $a_2$  and  $a_3$ . Parameters of (a) except:  $\omega_3 = 2.05$

**Fig. 9** Frequency-response curves of the 1:2:2 internal resonance for a low-frequency excitation ( $\Omega = \omega_1 + \sigma$ ). Variation of internal detuning when the solutions present unstable branches (- -).

(a) Parameters:  $\omega_1 = 1$ ,  $\omega_2 = 2.02$ ,  $\omega_3 = 2.03$ ,  $\mu_{1,2,3} = 0.1$ ,  $\alpha_{1,2,3,4} = 0.1$ ,  $F_1 = 0.1$ . (b) Parameters of (a) except:  $\omega_3 = 2.06$



Once again, similarities with the well-known 1:2 internal resonance are noted. But contrary to the 1:2:4 case, here the two 1:2 internal resonances are totally nested.

### 3.3 High-frequency excitation

In this last section, the external forcing is in the vicinity of the two high-frequency modes:

$$\Omega = \omega_2 + \epsilon\sigma = \omega_3 + \epsilon(\sigma + \sigma_1 - \sigma_2). \quad (48)$$

We also consider the case  $F_2 \neq 0$  and  $F_3 \neq 0$ , as in a real experiment, it is almost impossible to enforce either  $F_2 = 0$  or  $F_3 = 0$ . This leads to subharmonic resonance responses as

$$q_1 = a_1 \cos\left(\frac{\Omega}{2}t + \phi_1\right), \quad (49a)$$

$$q_2 = a_2 \cos(\Omega t + \phi_2), \quad (49b)$$

$$q_3 = a_3 \cos(\Omega t + \phi_2), \quad (49c)$$

where  $\phi_1 = -(\gamma + \gamma_1)/2$ ,  $\phi_2 = -\gamma$  and  $\phi_3 = -\gamma - \gamma_1 + \gamma_2$ .

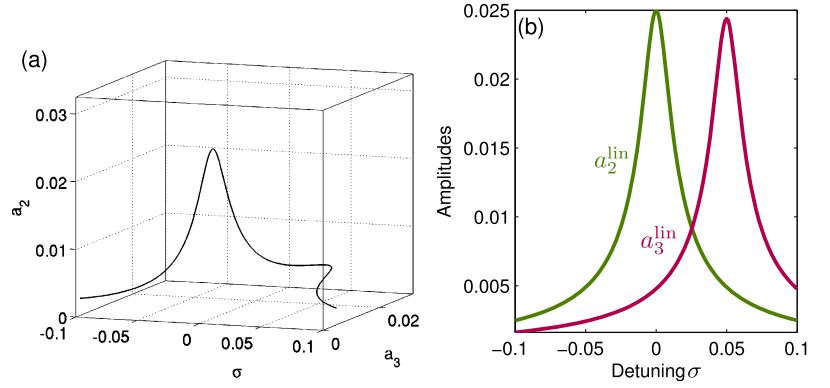
Including the angle relationships (Eq. 40) in the multiple scales method, the corresponding fixed points system reads:

$$-\mu_1 a_1 - \frac{\alpha_1 a_1 a_2}{4\omega_1} \sin(\gamma_1) - \frac{\alpha_2 a_1 a_3}{4\omega_1} \sin(\gamma_2) = 0, \quad (50a)$$

$$\begin{aligned} \sigma_1 + \frac{\alpha_3 a_1^2}{4\omega_2 a_2} \cos(\gamma_1) - \frac{\alpha_1 a_2}{2\omega_1} \cos(\gamma_1) - \frac{\alpha_2 a_3}{2\omega_1} \cos(\gamma_2) \\ - \frac{F_2}{2\omega_2 a_2} \cos(\gamma) = 0, \end{aligned} \quad (50b)$$

**Fig. 10**

Frequency-response curves of the 1:2:2 internal resonance for a high-frequency excitation case ( $\Omega = \omega_2 + \sigma$ ). Uncoupled responses: (a) in a 3D-space ( $\sigma, a_2, a_3$ ). (b) Projections onto ( $\sigma, a_2$ ) and ( $\sigma, a_3$ ). Selected values:  $\omega_1 = 1, \omega_2 = 2, \omega_3 = 2.05, \mu_{1,2,3} = 0.1, \alpha_{1,2,3,4} = 0.1, F_2 = F_3 = 0.001$



$$-\mu_2 a_2 + \frac{\alpha_3 a_1^2}{4\omega_2} \sin(\gamma_1) + \frac{F_2}{2\omega_2} \sin(\gamma) = 0, \quad (50c)$$

$$\sigma_2 + \frac{\alpha_4 a_1^2}{4\omega_3 a_3} \cos(\gamma_2) - \frac{\alpha_1 a_2}{2\omega_1} \cos(\gamma_1) - \frac{\alpha_2 a_3}{2\omega_1} \cos(\gamma_2) - \frac{F_3}{2\omega_3 a_3} \cos(\gamma + \gamma_1 - \gamma_2) = 0, \quad (50d)$$

$$-\mu_3 a_3 + \frac{\alpha_4 a_1^2}{4\omega_3} \sin(\gamma_2) + \frac{F_3}{2\omega_3} \sin(\gamma + \gamma_1 - \gamma_2) = 0, \quad (50e)$$

$$\sigma - \frac{\alpha_3 a_1^2}{4\omega_2 a_2} \cos(\gamma_1) + \frac{F_2}{2\omega_2 a_2} \cos(\gamma) = 0. \quad (50f)$$

System (50a)–(50f) presents six equations for six unknowns, however, a combination of the angles  $\gamma + \gamma_1 - \gamma_2$  appears in Eqs. (50d)–(50e), hence rendering a complete analytical solution untractable. Note that this ill-conditioning of the system appears to be intrinsic and cannot be eliminated through other relationships on angles. However, this ill-conditioning disappears if one lets either  $F_2 = 0$  or  $F_3 = 0$ ; and one is led to a most simple case for the stability condition, where a classical 1:2 is recovered. Fortunately, for our case with  $F_2 \neq 0$  and  $F_3 \neq 0$ , uncoupled solutions along with their stability analysis lend themselves to an analytical investigation given in the next subsection.

### 3.3.1 Uncoupled solutions

Analysis of the possible solutions of Eqs. (50a)–(50f) shows that two types of solutions are possible:

- (i) the uncoupled solutions where the directly excited modes  $q_2$  and  $q_3$  vibrate and  $q_1$  stays at rest ( $a_1 = 0$ ).
- (ii) the coupled solution where  $a_1, a_2$ , and  $a_3 \neq 0$ .

In case (i), combinations of Eqs. (50c) and (50f) and Eqs. (50e), (50b), and (50d), allow to derive the expressions of the uncoupled amplitudes  $a_2$  and  $a_3$  as

$$\begin{aligned} a_2^{\text{lin}} &= \frac{F_2}{2\omega_2 \sqrt{\mu_2^2 + \sigma^2}}, \\ a_3^{\text{lin}} &= \frac{F_3}{2\omega_3 \sqrt{\mu_3^2 + (\sigma + \sigma_1 - \sigma_2)^2}}. \end{aligned} \quad (51)$$

These solutions are denoted as  $(a_2^{\text{lin}}, a_3^{\text{lin}})$  since  $q_1 = 0$  in Eqs. (37a)–(37c) implies linear oscillator equations for  $q_2$  and  $q_3$ . Hence, the solutions found are those of a linear oscillator equation.

In this high-frequency excitation case, the two high-frequency modes are simultaneously excited ( $\Omega \approx \omega_2 \approx \omega_3$ ). Hence, the fundamental solution, from which stability has to be computed with respect to perturbations brought by the presence of the first oscillator, corresponds to a two-dofs system. This renders the analysis more complicated than the one led in all other cases studied in this paper. Consequently, stability analysis and representations of instability regions are conducted in the space  $(\sigma, a_2, a_3)$ . Figure 10(a) shows the uncoupled solution in that space. It consists of a single branch with two peaks corresponding to the linear resonances. Figure 10(b) shows the two projections of this solution branch on  $(\sigma, a_2)$  and  $(\sigma, a_3)$ .

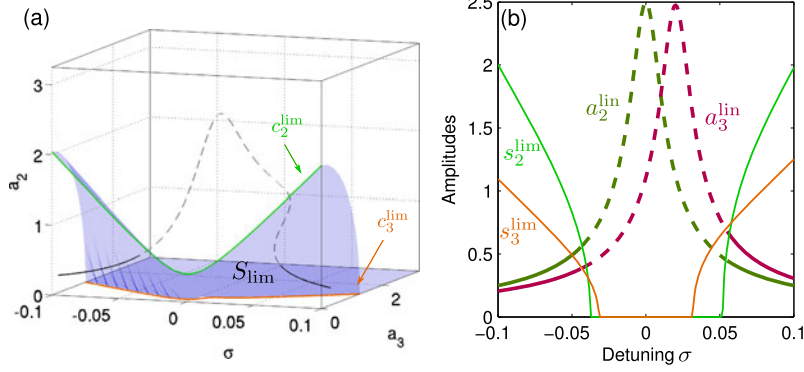


**Fig. 11** Frequency-response curves of the 1:2:2 internal resonance for a high-frequency excitation case ( $\Omega = \omega_2 + \varepsilon\sigma$ ). (a) 3D stability surface and intersections  $c_2^{\text{lim}} = S_{\text{lim}} \cap \{a_3 = 0\}$

and  $c_3^{\text{lim}} = S_{\text{lim}} \cap \{a_2 = 0\}$ . (b) 2D stability curves  $s_2^{\text{lim}}$  and  $s_3^{\text{lim}}$ . Unstable solutions (---). Selected values:  $\omega_1 = 1$ ,  $\omega_2 = 2$ ,  $\omega_3 = 2.02$ ,  $\mu_{1,2,3} = 0.1$ ,  $\alpha_{1,2,3,4} = 0.1$ ,  $F_2 = F_3 = 0.1$

### 3.3.2 Stability limit and coupling range

In order to study the stability of the linear solutions  $a_2^{\text{lin}}$  and  $a_3^{\text{lin}}$ , the Jacobian matrix of the fixed points system is calculated. The analytical expression is given in Appendix B.2.

The Jacobian is separable in this case and the six corresponding eigenvalues are easily found to be

$$\lambda_{1,2} = -\mu_2 \pm i\sigma, \quad (52a)$$

$$\lambda_{3,4} = -\mu_3 \pm i(\sigma_2 - \sigma_1 - \sigma), \quad (52b)$$

$$\lambda_5 = -\mu_1 - \frac{\alpha_1}{4\omega_1} a_2 \sin(\gamma_1) - \frac{\alpha_2}{4\omega_1} a_3 \sin(\gamma_2), \quad (52c)$$

$$\lambda_6 = \frac{\alpha_1}{4\omega_1} a_2 \sin(\gamma_1) + \frac{\alpha_2}{4\omega_1} a_3 \sin(\gamma_2). \quad (52d)$$

Obviously, the first four eigenvalues dictate the stability of the linear uncoupled solutions with respect to perturbations brought by  $(a_2, a_3)$ . They indicate stability, the last two ( $\lambda_5, \lambda_6$ ) governing the stability with respect to the presence of the first oscillator.

With a nontrivial combination of the fixed points equations (explained in Appendix B.2), one is able to derive an instability criterion on the amplitudes  $(a_2, a_3)$  only, which is given via the definition of an instability surface  $S_{\text{lim}}$  in  $(\sigma, a_2, a_3)$ :

$$S_{\text{lim}} = \{(\sigma, a_2, a_3) \mid T_1 = T_2 a_2^2 + T_3 a_3^2\} \quad (53)$$

with

$$\begin{cases} T_1 = 4\omega_1^2(4\mu_1^2 + (\sigma_1 + \sigma)^2), \\ T_2 = \alpha_1^2, \\ T_3 = \alpha_2^2 + 2\alpha_1\alpha_2 \frac{\omega_3}{\omega_2} \frac{F_2}{F_3} \\ \quad \times \frac{\mu_2\mu_3 + \sigma(\sigma + \sigma_1 - \sigma_2)}{\mu_2^2 + \sigma^2}. \end{cases} \quad (54)$$

The stability condition is a surface  $S_{\text{lim}}$  defined by a functional relationship of the form  $f(\sigma, a_2, a_3) = 0$ . It is represented on Fig. 11(a) in space  $(\sigma, a_2, a_3)$ , together with the uncoupled branch  $(a_2^{\text{lin}}, a_3^{\text{lin}})$ . Once the amplitudes on the fundamental branch are larger than  $S_{\text{lim}}$ , then the uncoupled solution becomes unstable. An analogy with the 1:2 internal resonance can be derived by defining  $c_2^{\text{lim}}$  and  $c_3^{\text{lim}}$  as the intersections of  $S_{\text{lim}}$  with either  $a_3 = 0$  or  $a_2 = 0$ :  $c_2^{\text{lim}} = S_{\text{lim}} \cap \{a_3 = 0\} = \sqrt{T_1/T_2}$ ;  $c_3^{\text{lim}} = S_{\text{lim}} \cap \{a_2 = 0\} = \sqrt{T_1/T_3}$ ; see Fig. 11(a). One can remark that the expressions for  $c_2^{\text{lim}}$  is equivalent to the expression of the instability limit for the 1:2 and 1:2:4 case; see, e.g., Eqs. (13) and (18) defining  $I_a$  and  $I_b$  in Sect. 2.2. For  $c_3^{\text{lim}}$ , an equivalent expression is found by imposing also  $F_2 = 0$  so as to recover a 1:2 resonance without the presence of the second oscillator.

In order to define a simple criterion on  $a_2^{\text{lin}}$  and  $a_3^{\text{lin}}$  independently, substituting for Eq. (51) in Eq. (53), two stability conditions  $s_2^{\text{lim}}$  and  $s_3^{\text{lim}}$  can be defined

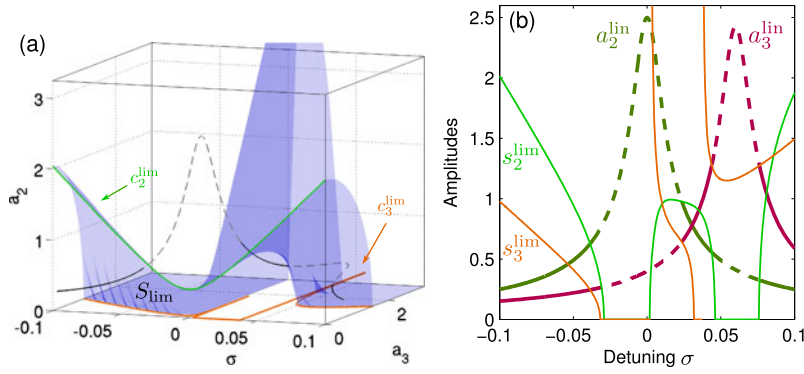


**Fig. 12** Frequency-response curves of the 1:2:2 internal resonance for a high-frequency excitation case ( $\Omega = \omega_2 + \varepsilon\sigma$ ). Variation of internal detuning  $\sigma_2$  and stability consequence. Unstable solutions (- -).

(a) 3D representation. (b) Corresponding 2D representation. Selected parameters:  $\omega_1 = 1$ ,  $\omega_2 = 2$ ,  $\omega_3 = 2.06$ ,  $\mu_{1,2,3} = 0.1$ ,  $\alpha_{1,2,3,4} = 0.1$ ,  $F_2 = F_3 = 0.1$

as

$$s_2^{\text{lim}} = \sqrt{\frac{T_1 - T_3(a_3^{\text{lin}})^2}{T_2}}, \quad \text{and} \quad (55)$$

$$s_3^{\text{lim}} = \sqrt{\frac{T_1 - T_2(a_2^{\text{lin}})^2}{T_3}}.$$

With that respect, one can check the stability for  $a_2$  and  $a_3$  with a simple scalar condition:  $a_2$  is stable if  $a_2^{\text{lin}} < s_2^{\text{lim}}$  (respectively,  $a_3$  is stable if  $a_3^{\text{lin}} < s_3^{\text{lim}}$ ). This is illustrated on Fig. 11(b) where  $s_2^{\text{lim}}$  and  $s_3^{\text{lim}}$  are represented on two-dimensional projections on  $(\sigma, a_2)$  and  $(\sigma, a_3)$ , defining easily the unstable region of the fundamental solution branch. Due to the complicated functional dependence of  $T_1$  and  $T_3$  with the parameters,  $s_2^{\text{lim}}$  and  $s_3^{\text{lim}}$  may have a complex shape, with at worst singular points due to a vanishing value for  $T_3$ . It is also important to note that, contrary to a simple 1:2 resonance, in this case  $s_2^{\text{lim}}$  and  $s_3^{\text{lim}}$  are dependent on forcing  $F_2$  and  $F_3$  (via  $T_3$ ).

Figure 12 shows a more complicated case, which has been obtained by increasing  $\sigma_2$  to 0.06. This leads to shift the resonance for  $a_3$  at a higher frequency as compared to Fig. 11. One can remark that  $c_2^{\text{lim}}$  has a simple expression, which lends it unconcerned with singularities. On the other hand, the expression of  $c_3^{\text{lim}}$  encounters singularities in that case due to two vanishing points for  $T_3$ ; see Fig. 12(a). In turn, the shape of  $S_{\text{lim}}$  becomes complex as it always have to join  $c_2^{\text{lim}}$  to  $c_3^{\text{lim}}$ . In the projections onto the planes  $(\sigma, a_2)$  and  $(\sigma, a_3)$ , represented in Fig. 12(b), one can see that the tangled shape of  $S_{\text{lim}}$  leads to complex behaviors for

stable solutions (- -). Nonetheless, the scalar stability condition still applies. However, one must take care of the fact that when  $T_3 < 0$ , which happens here between the two singular points, respectively  $\sigma = 0.0024$  and  $\sigma = 0.0044$ , the stability for  $a_3$  is inverted so as to take into account the negative sign (it remains unchanged for  $a_2$  as  $s_2^{\text{lim}}$  is not prone to singularities). This is more clearly seen on the 3D-plot, Fig. 12(a), where the part of the branch for  $\sigma \in [0.023, 0.043]$  lies under  $S_{\text{lim}}$ , and is thus stable.

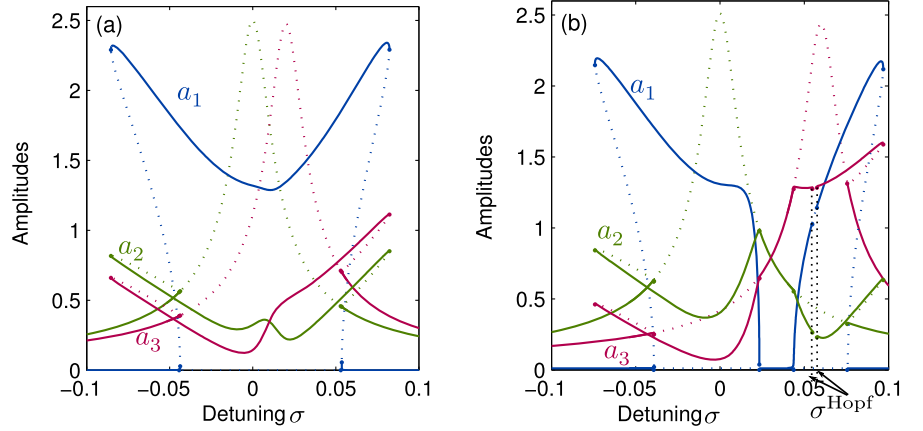
This investigation highlights the complexity brought by the presence of two oscillators in the high-frequency as compared to a simple 1:2 internal resonance. The instability limit can be changed significantly because of the possible complex behavior of  $T_3$ , and thus  $s_3^{\text{lim}}$ . It may lead, as in Fig. 12, to a stable portion of uncoupled solutions in between two unstable states, a feature that is not possible with a 1:2 resonance.

### 3.3.3 Coupled solutions

Fully coupled solutions with  $a_1 \neq 0$ ,  $a_2 \neq 0$ , and  $a_3 \neq 0$  for Eqs. (50a)–(50f) have not been derived, analytical expressions are not at hand. They may be derived from the system through complex trigonometric manipulations. However, analytical expressions are convenient when they are simple and prone to physical interpretations, and here their expressions would cover pages. Hence, only numerical solutions are shown here, allowing also to check the stability analysis of the previous section.



**Fig. 13** Numerical solutions: MANLab computation. 2D representation. Unstable solutions ( $\cdots$ ). (a) Unstable linear curves and coupled solutions. Parameters of Fig. 11 ( $\sigma_2 = 0.02$ ). (b) Multiple frequency ranges of coupling. Parameters of Fig. 12 ( $\sigma_2 = 0.06$ )



A continuation method is used to find numerically the periodic orbits of the forced system. Continuation is performed thanks to an Asymptotic-Numerical Method (ANM) implemented in the software MANLAB [9, 14], and stability is computed via Hill's method [15].

Two examples are proposed on Fig. 13, with the parameters selected for Figs. 11 and 12. In Fig. 13(a) (parameters of Fig. 11), the stability condition is verified and the transfer of energy from the uncoupled to the coupled solution is retrieved. The second case, displayed on Fig. 13(b), corresponds to the parameters of Fig. 12. Once again, the stability analysis is perfectly retrieved with the appearance of the stable state in the middle of the frequency range. As  $\sigma_2$  has been increased, this case resembles a succession of two 1:2 internal resonance between  $(q_1, q_2)$  and  $(q_1, q_3)$ , with a return to an uncoupled state in between. Finally, a very narrow interval of unstable coupled solutions are numerically found around  $\sigma \simeq 0.056$ , delimited by two Hopf bifurcations. This frequency range increases for larger values of the forcing amplitude, so that a broader occurrence of quasiperiodic solutions is found for higher nonlinearity.

### 3.4 Conclusion on the 1:2:2 resonance

In this section, a detailed analysis of the 1:2:2 internal resonance has been proposed. The study of the two excitation cases  $\Omega \simeq \omega_1$  and  $\Omega \simeq \omega_2 \simeq \omega_3$  has been done. In the high-frequency case, only the linear step is analytically solved, but a numerical

method is proposed in order to give the coupled solutions.

Some particularities are exhibited due to the interaction between the two high-frequency modes, but once again, the global behavior of the 1:2 internal resonance has been recovered.

In the low-frequency case, the energy is immediately and simultaneously transferred from  $a_1$  to  $a_2$  and  $a_3$ . For the high-frequency case, the limit of the stability can be understood as a surface represented in a 3D-space. Compared to the 1:2:4 internal resonance (part 1), there is no cascade of energy, but two nested 1:2 resonances.

Finally, contrary to the simple 1:2 internal resonance, the presence of a third oscillator can lead to Hopf bifurcation with quasiperiodic regime in coupled solutions even in the high-frequency case of excitation.

## 4 Conclusion

In this paper, a detailed analysis of two 3-dofs quadratic nonlinear systems presenting internal resonances, has been proposed. These models are two combinations of the well-known 1:2 internal resonance. Forced oscillations are considered and the systems are expressed under their normal form. In each case, an external forcing is applied on each oscillator equation.

For the 1:2:4 resonance, it has been shown that it may be interpreted as a cascade of two 1:2 internal resonances. When  $\Omega \simeq \omega_3$ , two components oscillat-



ing at  $\Omega/2$  and  $\Omega/4$  are created by the first and second oscillators. Energy can be transferred in a two-stage process, first to the second mode, and finally for the first one. The two stability conditions for these different regimes have been exhibited and resembles the stability limit for a classical 1:2 resonance. Finally, it has been found that the presence of the first oscillator leads to the occurrence of Hopf bifurcations in the fully coupled regime so that quasiperiodic responses are favored. When  $\Omega \simeq \omega_2$ , two components are created oscillating at  $\Omega/2$  and  $2\Omega$ . The system can be analyzed as composed of two 1:2 resonances, both excited in its lower and its higher frequency at the same time. The last case ( $\Omega \simeq \omega_1$ ) leads to two components oscillating at  $2\Omega$  and  $4\Omega$ . As in the 1:2 case, there is no stability limit, the energy is directly transferred to the two upper frequency modes. As compared to the 1:2 case, it has been found that quasiperiodic regimes are more easily observed.

The second model, displaying a 1:2:2 resonance, can be seen as two nested 1:2 internal resonances. When  $\Omega \simeq \omega_1$ , the solutions present a lot of similarities with the 1:2 case. Amplitudes solutions are locally affected by the third oscillator, however the global behavior of a 1:2 resonance is recovered. For the last case ( $\Omega \simeq 2\omega_1$ ), a stability condition has been derived and it has been demonstrated how the shape of the instability region can become complex for certain parameter values. Fully coupled solutions are not analytically tractable in the case considered so that numerical solutions have been exhibited, and once again Hopf bifurcations have been observed on the fully coupled branches.

A general conclusion that can be drawn out, as compared to the simple 1:2 resonance, is that the presence of a third oscillator favors unstable states for fully coupled regions so that quasiperiodic regimes become more generic.

## Appendix A: Analytical expressions for the 1:2:4 internal resonance

### A.1 1:2:4 mid-frequency case

Jacobian matrix of system (25a)–(25f), with  $a_1 = 0$ :

$$\mathcal{J} = \begin{pmatrix} -\mu_1 + \frac{\alpha_1 a_2}{4\omega_1} \sin(\gamma_1) & 0 & 0 \\ 0 & -\frac{\alpha_1 a_2}{2\omega_1} \sin(\gamma_1) & \frac{\alpha_1}{2\omega_1} \cos(\gamma_1) + \frac{F_2}{2\omega_2 a_2^2} \cos(\gamma) \\ 0 & 0 & -\mu_2 + \frac{\alpha_3 a_3}{4\omega_2} \sin(\gamma_2) \\ 0 & 0 & -\frac{F_2}{2\omega_2 a_2^2} \cos(\gamma) \\ 0 & 0 & -\frac{\alpha_4 a_2}{2\omega_3} \sin(\gamma_2) \\ 0 & 0 & -\frac{\alpha_4 a_2}{2\omega_3 a_3} \cos(\gamma_2) - \frac{F_2}{\omega_2 a_2^2} \cos(\gamma) \\ 0 & 0 & 0 \\ \frac{F_2}{2\omega_2 a_2} \sin(\gamma) & -\frac{\alpha_3}{4\omega_2} \cos(\gamma_2) & \frac{\alpha_3 a_3}{4\omega_2} \sin(\gamma_2) \\ \frac{F_2}{2\omega_2} \cos(\gamma) & \frac{\alpha_3 a_2}{4\omega_2} \sin(\gamma_2) & \frac{\alpha_3 a_3 a_2}{4\omega_2} \cos(\gamma_2) \\ -\frac{F_2}{2\omega_2 a_2} \sin(\gamma) & \frac{\alpha_3}{4\omega_2} \cos(\gamma_2) & -\frac{\alpha_3 a_3}{4\omega_2} \sin(\gamma_2) \\ 0 & -\mu_3 & -\frac{\alpha_4 a_2^2}{4\omega_3} \cos(\gamma_2) \\ -\frac{F_2}{\omega_2 a_2} \sin(\gamma) & \frac{\alpha_4 a_2^2}{4\omega_3 a_3} \cos(\gamma_2) + \frac{\alpha_3}{2\omega_2} \cos(\gamma_2) & \frac{\alpha_4 a_2^2}{4\omega_3 a_3} \sin(\gamma_2) - \frac{\alpha_3 a_3}{2\omega_2} \sin(\gamma_2) \end{pmatrix}.$$

The coefficients of the five-order polynomial of  $a_2^2$  (see Eq. (36)) are given by

$$\left\{ \begin{array}{l} C_{10} = \frac{\alpha_3^2 \alpha_1^4 \alpha_4^2}{16^3 \alpha_2^2 \omega_1^4 \omega_3^2 (\mu_3^2 + \nu_3^2)}, \\ C_8 = \frac{\omega_2 \alpha_3 \alpha_1^4 \alpha_4}{27 \alpha_2^2 \omega_1^4 \omega_3} \frac{(\mu_2 \mu_3 - \nu_2 \nu_3)}{(\mu_3^2 + \nu_3^2)} + \frac{\alpha_3^2 \alpha_1^2 \alpha_4^2}{128 \alpha_2^2 \omega_1^2 \omega_3^2} \frac{(\mu_1^2 + \nu_1^2)}{(\mu_3^2 + \nu_3^2)} - \frac{\alpha_3^2 \alpha_1^2 \alpha_4^2}{4^3 \alpha_2^2 \omega_1^2 \omega_3^2} \frac{(\nu_1 \nu_3 - \mu_1 \mu_3)^2}{(\mu_3^2 + \nu_3^2)^2}, \\ C_6 = \frac{\omega_2^2 \alpha_1^4}{16 \alpha_2^2 \omega_1^4} (\mu_2^2 + \nu_2^2) + \frac{\omega_2 \alpha_3 \alpha_1^2 \alpha_4}{4 \alpha_2^2 \omega_1^2 \omega_3} \frac{(\mu_1^2 + \nu_1^2)(\mu_2 \mu_3 - \nu_2 \nu_3)}{(\mu_3^2 + \nu_3^2)} + \frac{\alpha_3^2 \alpha_4^2}{16 \alpha_2^2 \omega_3^2} \frac{(\mu_1^2 + \nu_1^2)^2}{(\mu_3^2 + \nu_3^2)} \\ + \frac{\alpha_1^2 \alpha_3 \alpha_4 \omega_2}{2 \alpha_2^2 \omega_3 \omega_1^2} \frac{(\mu_1 \mu_2 + \nu_1 \nu_2)(\nu_1 \nu_3 - \mu_1 \mu_3)}{(\mu_3^2 + \nu_3^2)}, \\ C_4 = \frac{2 \omega_2^2 \alpha_1^2}{\alpha_2^2 \omega_1^2} (\mu_2^2 + \nu_2^2)(\mu_1^2 + \nu_1^2) - \frac{4 \omega_2^2 \alpha_1^2}{\alpha_2^2 \omega_1^2} (\mu_1 \mu_2 + \nu_1 \nu_2) - \frac{F_1^2 \alpha_1 \alpha_3 \alpha_4}{16 \alpha_2 \omega_3 \omega_1^3} \frac{(\nu_1 \nu_3 - \mu_1 \mu_3)}{(\mu_3^2 + \nu_3^2)} \\ + \frac{2 \alpha_3 \alpha_4 \omega_2}{\alpha_2^2 \omega_3} \frac{(\mu_1^2 + \nu_1^2)^2 (\mu_2 \mu_3 - \nu_2 \nu_3)}{(\mu_3^2 + \nu_3^2)}, \\ C_2 = \frac{16 \omega_2^2}{\alpha_2^2} (\mu_1^2 + \nu_1^2)^2 (\mu_2^2 + \nu_2^2) + \frac{F_1^2 \alpha_1 \omega_2}{\alpha_2 \omega_1^3} (\nu_1 \nu_2 + \mu_1 \mu_2), \\ C_0 = -\frac{F_1^4}{16 \omega_1^4}. \end{array} \right.$$

The Jacobian matrix associated to Eqs. (33a)–(33f) reads

$$\mathcal{J} = \begin{pmatrix} -\mu_1 + \frac{\alpha_1 a_2}{4 \omega_1} \sin(\gamma_1) & \frac{F_1}{2 \omega_1} \cos(\gamma) & \frac{\alpha_1 a_1 a_2}{4 \omega_1} \cos(\gamma_1) \\ -\frac{Q_1}{2 \omega_1 a_1^2} \cos(\gamma) & -\frac{F_1}{2 \omega_1 a_1} \sin(\gamma) & \frac{\alpha_1}{4 \omega_1} \cos(\gamma_1) \\ -\frac{\alpha_2 a_1}{2 \omega_2} \sin(\gamma_1) & 0 & -\mu_2 + \frac{\alpha_3 a_3}{4 \omega_2} \sin(\gamma_2) \\ -\frac{\alpha_2 a_1}{2 \omega_2 a_2} \cos(\gamma_1) - \frac{F_1}{\omega_1 a_1^2} \cos(\gamma) & -\frac{F_1}{\omega_1 a_1} \sin(\gamma) & \frac{\alpha_2 a_1^2}{4 \omega_2 a_2^2} \cos(\gamma_1) + \frac{\alpha_1}{2 \omega_1} \cos(\gamma_1) \\ 0 & 0 & -\frac{\alpha_4 a_2}{2 \omega_3} \sin(\gamma_2) \\ \frac{\alpha_2 a_1}{\omega_2 a_2} \cos(\gamma_1) & 0 & -\frac{\alpha_4 a_2}{2 \omega_3 a_3} \cos(\gamma_2) - \frac{\alpha_2 a_1^2}{2 \omega_2 a_2^2} \cos(\gamma_1) \\ 0 & 0 & 0 \\ -\frac{\alpha_1 a_2}{4 \omega_1} \sin(\gamma_1) & 0 & 0 \\ -\frac{\alpha_2 a_1^2}{4 \omega_2} \cos(\gamma_1) & \frac{\alpha_3 a_2}{4 \omega_2} \sin(\gamma_2) & \frac{\alpha_3 a_3 a_2}{4 \omega_2} \cos(\gamma_2) \\ \frac{\alpha_2 a_1^2}{4 \omega_2 a_2} \sin(\gamma_1) - \frac{\alpha_1 a_2}{2 \omega_1} \sin(\gamma_1) & -\frac{\alpha_3}{4 \omega_2} \cos(\gamma_2) & \frac{\alpha_3 a_3}{4 \omega_2} \sin(\gamma_2) \\ 0 & -\mu_3 & -\frac{\alpha_4 a_2^2}{4 \omega_3} \cos(\gamma_2) \\ -\frac{\alpha_2 a_1^2}{2 \omega_2 a_2} \sin(\gamma_1) & \frac{\alpha_4 a_2^2}{4 \omega_3 a_3^2} \cos(\gamma_2) + \frac{\alpha_3}{2 \omega_2} \cos(\gamma_2) & \frac{\alpha_4 a_2^2}{4 \omega_3 a_3} \sin(\gamma_2) - \frac{\alpha_3 a_3}{2 \omega_2} \sin(\gamma_2) \end{pmatrix}.$$

---

## Appendix B: Jacobian matrices for the 1:2:2 internal resonance

### B.1 1:2:2 low-frequency case

Jacobian matrix associated to Eqs. (43a)–(43f):

$$\mathcal{J} = \begin{pmatrix} -\mu_1 - \frac{\alpha_1 a_2}{4\omega_1} \sin(\gamma_1) - \frac{\alpha_2 a_3}{4\omega_1} \sin(\gamma_2) & -\frac{\alpha_1 a_1 a_2}{4\omega_1} \cos(\gamma_1) & -\frac{\alpha_1 a_1}{4\omega_1} \sin(\gamma_1) \\ \frac{\alpha_3 a_1}{2\omega_2 a_2} \cos(\gamma_1) - \frac{F_1}{\omega_1 a_1^2} \cos(\gamma) & -\frac{\alpha_3 a_1^2}{4\omega_2} \sin(\gamma_1) + \frac{\alpha_1 a_2}{2\omega_1} \sin(\gamma_1) & -\frac{\alpha_1}{2\omega_1} \cos(\gamma_1) - \frac{\alpha_3 a_1^2}{4\omega_2 a_2^2} \cos(\gamma_1) \\ \frac{\alpha_3 a_1}{2\omega_2} \sin(\gamma_1) & \frac{\alpha_3 a_1^2}{4\omega_2} \cos(\gamma_1) & -\mu_2 \\ \frac{\alpha_4 a_1}{2\omega_3 a_3} \cos(\gamma_2) - \frac{F_1}{\omega_1 a_1^2} \cos(\gamma) & \frac{\alpha_1 a_2}{2\omega_1} \sin(\gamma_1) & -\frac{\alpha_1}{2\omega_1} \cos(\gamma_1) \\ \frac{\alpha_4 a_1}{2\omega_3} \sin(\gamma_2) & 0 & 0 \\ -\frac{F_1}{2\omega_1 a_1^2} \cos(\gamma) & \frac{\alpha_1 a_2}{4\omega_1} \sin(\gamma_1) & -\frac{\alpha_1}{4\omega_1} \cos(\gamma_1) \\ -\frac{\alpha_2 a_1 a_3}{4\omega_1} \cos(\gamma_2) & -\frac{\alpha_2 a_1}{4\omega_1} \sin(\gamma_2) & \frac{F_1}{2\omega_1} \cos(\gamma) \\ \frac{\alpha_2 a_3}{2\omega_1} \sin(\gamma_2) & -\frac{\alpha_2}{2\omega_1} \cos(\gamma_2) & -\frac{F_1}{\omega_1 a_1} \sin(\gamma) \\ 0 & 0 & 0 \\ -\frac{\alpha_4 a_1^2}{4\omega_3 a_3} \sin(\gamma_2) + \frac{\alpha_2 a_3}{2\omega_1} \sin(\gamma_2) & -\frac{\alpha_2}{2\omega_1} \cos(\gamma_2) - \frac{\alpha_4 a_1^2}{4\omega_3 a_3^2} \cos(\gamma_2) & -\frac{F_1}{\omega_1 a_1} \sin(\gamma) \\ \frac{\alpha_4 a_1^2}{4\omega_3} \cos(\gamma_2) & -\mu_3 & 0 \\ \frac{\alpha_2 a_3}{4\omega_1} \sin(\gamma_2) & -\frac{\alpha_2}{4\omega_1} \cos(\gamma_2) & -\frac{F_1}{\omega_1 a_1} \sin(\gamma) \end{pmatrix}.$$

### B.2 1:2:2 high-frequency

Jacobian matrix associated to Eqs. (50a)–(50f):

$$\mathcal{J} = \begin{pmatrix} -\mu_1 - \frac{\alpha_1 a_2}{4\omega_1} \sin(\gamma_1) - \frac{\alpha_2 a_3}{4\omega_1} \sin(\gamma_2) & 0 & 0 \\ 0 & \frac{\alpha_1 a_2}{2\omega_1} \sin(\gamma_1) & \frac{F_2}{2\omega_2 a_2^2} \cos(\gamma) - \frac{\alpha_1}{2\omega_1} \cos(\gamma_1) \\ 0 & 0 & -\mu_2 \\ 0 & \frac{\alpha_1 a_2}{2\omega_1} \sin(\gamma_1) + \frac{F_3}{2\omega_3 a_3} \sin(\gamma + \gamma_1 - \gamma_2) & -\frac{\alpha_1}{2\omega_1} \cos(\gamma_1) \\ 0 & \frac{F_3}{2\omega_3} \cos(\gamma + \gamma_1 - \gamma_2) & 0 \\ 0 & 0 & -\frac{F_2}{2\omega_2 a_2^2} \cos(\gamma) \\ 0 & 0 & 0 \\ \frac{\alpha_2 a_3}{2\omega_1} \sin(\gamma_2) & -\frac{\alpha_2}{2\omega_1} \cos(\gamma_2) & \frac{F_2}{2\omega_2 a_2} \sin(\gamma) \\ 0 & 0 & \frac{F_2}{2\omega_2} \cos(\gamma) \\ \frac{\alpha_2 a_3}{2\omega_1} \sin(\gamma_2) - \frac{F_3}{2\omega_3 a_3} \sin(\gamma + \gamma_1 - \gamma_2) & \frac{F_3}{2\omega_3 a_3^2} \cos(\gamma + \gamma_1 - \gamma_2) - \frac{\alpha_2}{2\omega_1} \cos(\gamma_2) & \frac{F_3}{2\omega_3 a_3} \sin(\gamma + \gamma_1 - \gamma_2) \\ -\frac{F_3}{2\omega_3} \cos(\gamma + \gamma_1 - \gamma_2) & -\mu_3 & \frac{F_3}{2\omega_3} \cos(\gamma + \gamma_1 - \gamma_2) \\ 0 & 0 & -\frac{F_2}{2\omega_2 a_2} \sin(\gamma) \end{pmatrix}.$$

The corresponding eigenvalues are computed as

$$\begin{cases} \lambda_{1,2} = -\mu_2 \pm i\sigma, \\ \lambda_{3,4} = -\mu_3 \pm i(\sigma_2 - \sigma_1 - \sigma), \\ \lambda_5 = -\mu_1 - \frac{\alpha_1}{4\omega_1}a_2 \sin(\gamma_1) - \frac{\alpha_2}{4\omega_1}a_3 \sin(\gamma_2), \\ \lambda_6 = \frac{\alpha_1}{4\omega_1}a_2 \sin(\gamma_1) + \frac{\alpha_2}{4\omega_1}a_3 \sin(\gamma_2). \end{cases} \quad (56)$$

The product  $\lambda_5 \lambda_6$  drives the stability of the solution. Searching for its cancellation points, one can see that it is equivalent to cancel the following expression:

$$\alpha_1 a_2 \sin \gamma_1 + \alpha_2 a_3 \sin \gamma_2 = -4\omega_1 \mu_1. \quad (57)$$

From Eqs. (50b) and (50f), another relationship between  $\gamma_1$  and  $\gamma_2$  is obtained:

$$\alpha_1 a_2 \cos \gamma_1 + \alpha_2 a_3 \cos \gamma_2 = 2\omega_1(\sigma_1 + \sigma). \quad (58)$$

The combination of Eqs. (58) and (57) leads to

$$\begin{aligned} 4\omega_1^2(4\mu_1^2 + (\sigma_1 + \sigma)^2) \\ = \alpha_1^2 a_2^2 + \alpha_2^2 a_3^2 + 2\alpha_1 \alpha_2 a_2 a_3 \cos(\gamma_1 - \gamma_2). \end{aligned} \quad (59)$$

$\cos(\gamma_1 - \gamma_2)$  is expressed thanks to Eqs. (50c) and (50f) as:

$$\cos(\gamma_1 - \gamma_2) = \frac{\omega_3 a_3}{\omega_2 a_2} \frac{F_2}{F_3} \frac{\mu_2 \mu_3 + \sigma(\sigma + \sigma_1 - \sigma_2)}{\mu_2^2 + \sigma^2}. \quad (60)$$

Finally, the stability condition is

$$S_{\text{lim}} = \{(\sigma, a_2, a_3) | T_1 = T_2 a_2^2 + T_3 a_3^2\} \quad (61)$$

where

$$\begin{cases} T_1 = 4\omega_1^2(4\mu_1^2 + (\sigma_1 + \sigma)^2), \\ T_2 = \alpha_1^2, \\ T_3 = \alpha_2^2 + 2\alpha_1 \alpha_2 \frac{\omega_3}{\omega_2} \frac{F_2}{F_3} \\ \quad \times \frac{\mu_2 \mu_3 + \sigma(\sigma + \sigma_1 - \sigma_2)}{\mu_2^2 + \sigma^2}. \end{cases} \quad (62)$$

## References

- Achong, A.: The steelpan as a system of non-linear mode-localized oscillators, I: theory, simulations, experiments and bifurcations. *J. Sound Vib.* **197**(4), 471–487 (1996)
- Achong, A.: The steelpan as a system of non-linear mode-localized oscillators, part III: the inverse problem—parameter estimation. *J. Sound Vib.* **212**(4), 623–635 (1998)
- Achong, A.: Mode locking on the non-linear notes of the steelpan. *J. Sound Vib.* **266**, 193–197 (2003)
- Achong, A., Sinanan-Singh, K.A.: The steelpan as a system of non-linear mode-localized oscillators, part II: coupled sub-systems, simulations and experiments. *J. Sound Vib.* **203**(4), 547–561 (1997)
- Amabili, M., Pellicano, F., Valakis, A.F.: Nonlinear vibrations and multiple resonances of fluid-filled, circular shells, part I: equations of motion and numerical results. *J. Vib. Acoust.* **122**, 346–354 (2000)
- Arnold, V.I., Levi, M., Szűcs, J.: Geometrical Methods in the Theory of Ordinary Differential Equations. Springer, Berlin (1988)
- Chaigne, A., Touzé, C., Thomas, O.: Nonlinear vibrations and chaos in gongs and cymbals. *Acoust. Sci. Technol.* **26**(5), 403–409 (2005)
- Chin, C.-M., Nayfeh, A.H.: A second-order approximation of multi-modal interactions in externally excited circular cylindrical shells. *Nonlinear Dyn.* **26**, 45–66 (2001)
- Cochelin, B., Vergez, C.: A high-order purely frequency-based harmonic balance formulation for continuation of periodic solutions. *J. Sound Vib.* **324**, 243–262 (2009)
- Froude, W.: Remarks on Mr. Scott Russell's paper on rolling. *Trans. Inst. Naval Research* **7**, 232–275 (1863)
- Haddow, A.G., Barr, A.D.S., Mook, D.T.: Theoretical and experimental study of modal interaction in two-degree-of-freedom structure. *J. Sound Vib.* **97**(3), 451–473 (1984)
- Hanson, R.J., Anderson, J.M., Macomber, H.K.: Measurements of nonlinear effects in a driven vibrating wire. *J. Acoust. Soc. Am.* **96**(3), 1549–1556 (1994)
- Iooss, G., Adelmeyer, M.: Topics in Bifurcation Theory. Advanced Series in Nonlinear Dynamics (1998)
- Karkar, S., Cochelin, B., Vergez, C., Thomas, O., Lazarus, A.: User guide Manlab 2.0. Technical report, Laboratoire de Mécanique et d'Acoustique (LMA), CNRS UPR 7051 (2012). <http://manlab.lma.cnrs-mrs.fr/>
- Lazarus, A., Thomas, O.: A harmonic-based method for computing the stability of periodic solutions of dynamical systems. *C. R., Méc.* **338**, 510–517 (2010)
- Lee, C., Perkins, N.C.: Three-dimensional oscillations of suspended cables involving simultaneous internal resonances. *Nonlinear Dyn.* **8**, 45–63 (1995)
- Miles, J.W.: Stability of forced oscillations of a vibrating string. *J. Acoust. Soc. Am.* **38**(5), 855–861 (1965)
- Miles, J.W.: Resonant, nonplanar motion of a stretched string. *J. Acoust. Soc. Am.* **75**(5), 1505–1510 (1984)
- Monteil, M., Touzé, C., Thomas, O.: Complicated dynamics exhibited by thin shells displaying numerous internal resonances: application to the steelpan. In: 19th International Congress on Sound and Vibrations (ICSV), Vilnius, Lithuania, 8–12 July 2012
- Myers, A., Pyle, R.W., Gilbert, J. Jr., Campbell, D.M., Chick, J.P., Logie, S.: Effects of nonlinear sound propagation on the characteristic timbres of brass instruments. *J. Acoust. Soc. Am.* **131**(1), 678–688 (2012)
- Nayfeh, A.H., Zavodney, L.D.: Experimental observation of amplitude and phase-modulated responses of two inter-

- 
- nally coupled oscillators to harmonic excitation. *J. Appl. Mech.* **55**, 706–710 (1988)
22. Nayfeh, A.H.: On the undesirable roll characteristics of ships in regular seas. *J. Ship Res.* **32**, 92–100 (1988)
  23. Nayfeh, A.H.: *Nonlinear Interactions*. Wiley, New York (2000)
  24. Nayfeh, A.H., Mook, D.T.: *Nonlinear Oscillations*. Wiley, New York (1979)
  25. Nayfeh, T.A., Asrar, W., Nayfeh, A.H.: Three-mode interactions in harmonically excited systems with quadratic nonlinearities. *Nonlinear Dyn.* **3**, 385–410 (1992)
  26. Nazarenko, S.: *Wave Turbulence*. Lecture Notes in Physics, vol. 825. Springer, Berlin (2011)
  27. Noreland, D., Bellizzi, S., Vergez, C., Bouc, R.: Nonlinear modes of clarinet-like musical instruments. *J. Sound Vib.* **324**(3–5), 983–1002 (2009)
  28. Pellicano, F., Amabili, M., Valakis, A.F.: Nonlinear vibrations and multiple resonances of fluid-filled, circular shells, part 2: perturbation analysis. *J. Vib. Acoust.* **122**, 355–364 (2000)
  29. Poincaré, H.: *Les Méthodes Nouvelles de la Mécanique Céleste*. Gauthiers-Villars, Paris (1892)
  30. Ruelle, D., Takens, F.: On the nature of turbulence. *Commun. Math. Phys.* **20**, 167–192 (1971)
  31. Sanders, J.A., Verhulst, F.: *Averaging Methods in Nonlinear Dynamical Systems* (1985) (revised ed. 2007)
  32. Thomas, O., Lazarus, A., Touzé, C.: A harmonic-based method for computing the stability of periodic oscillations of nonlinear structural systems. In: *ASME/IDETC 2010 (International Design Engineering Technical Conference)*, Montreal, Québec, Canada, 15–18 Aug. 2010
  33. Thomas, O., Touzé, C., Chaigne, A.: Non-linear vibrations of free-edge thin spherical shells: modal interaction rules and 1:1:2 internal resonance. *Int. J. Solids Struct.* **42**, 3339–3373 (2005)
  34. Thomas, O., Touzé, C., Luminais, E.: Non-linear vibrations of free-edge thin spherical shells: experiments on a 1:1:2 internal resonance. *Nonlinear Dyn.* **49**(1–2), 259–284 (2007)
  35. Tien, W.-M., Namachchivaya, N.S., Bajaj, A.K.: Non-linear dynamics of a shallow arch under periodic excitation, I: 1:2 internal resonance. *Int. J. Non-Linear Mech.* **23**(3), 349–366 (1994)
  36. Touzé, C., Bilbao, S., Cadot, O.: Transition scenario to turbulence in thin vibrating plates. *J. Sound Vib.* **331**, 412–433 (2012)
  37. Touzé, C., Thomas, O., Amabili, M.: Transition to chaotic vibrations for harmonically forced perfect and imperfect circular plates. *Int. J. Non-Linear Mech.* **46**(1), 234–246 (2011)
  38. Touzé, C., Thomas, O., Chaigne, A.: Hardening/softening behaviour in non-linear oscillations of structural systems using non-linear normal modes. *J. Sound Vib.* **273**, 77–101 (2004)